東北医科薬科大学

審査学位論文（博士）

氏名（本籍）	パン　　スンリ 潘　　順　麗　（中国）
学位の種類	博士（薬科学）
学位記番号	博薬学第 24 号
学位授与の日付	令和 6 年 3 月 8 日
学位授与の要件	学位規則第 4 条 1 項該当
学位論文題名	Each *N*-glycan on human IgA and J-chain uniquely affects oligomericity and stability （ヒト IgA および J 鎖の N-型糖鎖修飾が複合体形成や安定性に及ぼす影響）
論文審査委員	主査　　教 授　顧　　建国
	副査　　教 授　藤村　　務
	副査　　教 授　山口　芳樹

Each *N*-glycan on human IgA and J-chain uniquely affects oligomericity and stability

東北医科薬科大学大学院薬学研究科

博士後期課程

糖鎖構造生物学教室

潘 順 麗

Contents

1. Introduction

Immunoglobulin A (IgA) is the most abundant immunoglobulin and its production exceeds that of the sum of the other immunoglobulins. IgA occurs as a monomer in serum or is assembled into dimers or polymers with joining chain (J-chain) [1]. Polymeric IgA can be transported to the mucosal surface by binding to the secretory component (SC) of the polymeric Ig receptor (pIgR), and is then known as secretory IgA (sIgA) [2, 3]. The main molecular form of sIgA is dimeric, although some higher order IgA oligomers do occur including trimers, tetramers and pentamers [4]. The dimeric IgA is formed through intermolecular disulfide bridges between the Fc tail (Cys471) and the J-chain (Cys15 or Cys69). Assembly into higher order polymers involves another IgA monomer that binds via two unpaired Cys471 residues [5]. IgA differs from IgG in that it is characteristically employed in recruiting polymorphonuclear cells, in multivalent antigen binding, in FcαRI-mediated cytotoxicity, in mucosal immune response and in the development of bispecific antibodies (BsAb) [6-9]. This diversity provides more possibilities for the therapeutic use of IgA antibodies. Consequently, there is growing interest in the structure-function relationships of IgA, with recent reports of atomic-scale structural information of IgA-Fc, providing insights into the modes of molecular assembly [5, 10, 11].

Glycosylation affects many of the properties of immunoglobulin G (IgG). The *N*-glycan at N297 of the Fc region contributes to its structural integrity [12]. Removal of the fucose residue increases binding affinity to the Fcγ receptor, and enhances the downstream antibody-dependent cellular cytotoxicity [13]. However, little is known about the role of glycans attached onto other immunoglobulin classes. Human IgA comprises two subclasses, IgA1 and IgA2. The hinge region of IgA1 is heavily glycosylated with GalNAc-type *O*-glycans and the aberrant glycoform of IgA1, deficient in galactosylation, leads to IgA nephropathy [14]. Both IgA1 and IgA2 have two common *N*-glycosylation sites, N263 in Cα2 and N459 in the tailpiece [14]. Alignment of the amino acid sequences shows that N459 is highly conserved [15, 16]

(Fig. 1A). N49 of the J-chain is also well conserved [17] (Fig. 1B). There are several

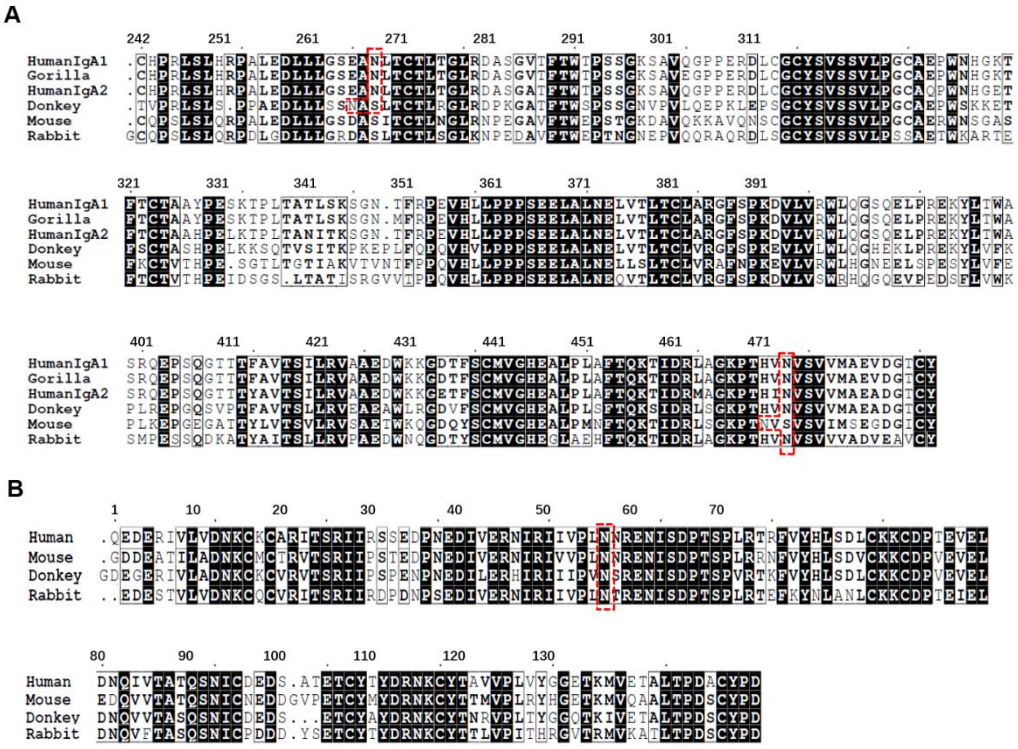

Figure 1. Amino acid sequence alignments of IgA-Fc and J-chain among different mammalian species.

Sequence alignment of IgA-Fc (A) and J-chain (B). Shadowed residues are conserved among the different species examined. Dotted boxes indicate *N*-glycosylation sites.

studies highlighting the role of IgA glycosylation in bacterial recognition. IgA *N*-glycan independently assists antibody-epitope recognition through interaction with Gram-positive and Gram-negative bacteria in the mucosal immune system [18, 19]. The mechanism may involve terminal monosaccharide residues of the sIgA *N*-glycans as potential binding sites for some respiratory and gastrointestinal pathogens [20, 21]. sIgA from colostrum inhibits local adhesion of enteropathogenic *Escherichia coli* (EPEC) by binding to EPEC adhesion factors via a fucose residue in IgA [22]. Infection with S-fimbriated *Escherichia coli*, a cause of sepsis and meningitis in neonates, may be prevented by the presence of sialylated glycans on sIgA [23]. Additionally, high sialylation of IgA antibodies extends the otherwise short *in vivo* half-life of native IgA

antibodies in mice [24].

There are limited studies focusing on the role of individual *N*-glycosylation on IgA and J-chain, and the results regarding the role of IgA *N*-glycosylation in binding to IgA Fc receptor FcαRI are contradictory. Removal of the N263-glycan brings about a moderate increase in binding to FcαRI [25] or a complete loss [26]. Recently, two groups independently found that the N459-glycan rather than the N263-glycan contributes to the interaction with FcαRI [27, 28]. Only a few studies explore the effect of *N*-glycans on assembly of IgA. Of these, one shows that N459 *N*-glycans do influence the polymerization of IgA [29], while another that the *N*-glycan of the J-chain plays a role in maintaining conformation, since mutation of mouse J-chain N49 prevents dimer formation of IgA [30]. Although partial 3D structural information on sIgA *N*-glycans is available [31], the determination of structure-function relationships of the *N*-glycans is just beginning. Such understanding will benefit development of both IgA antibody therapeutics and vaccines.

The structural and functional roles of *N*-glycosylation of the J-chain and IgA are here investigated by introducing mutations at N263 (Fc), N459 (Fc) and N49 (J-chain), either singly or in combination. IgA1-Fc and the complex with Fc-J-chain were expressed, purified, and characterized. Results are discussed in terms of a constructed 3D model of the *N*-glycosylated IgA-Fc-J-chain complex.

2. Materials and Methods

2.1 Construct design

Amino acid sequences of the human immunoglobulin heavy constant alpha 1 (IgA1) and human immunoglobulin joining chain (J-chain) were obtained from the UniProt database (P01876 and P01591). Insert DNAs were codon-optimized for mammalian expression and chemically synthesized by Thermo Fisher Scientific Inc. Genes encoding human IgA1-Fc (242-472) containing an N-terminal IL-2 signal sequence, FLAG tag (DYKDDDDK) and TEV protease site (ENLYFQ-G), were cloned into a pcDNA3.4 mammalian expression vector (Thermo Fisher Scientific). Genes encoding human full-length J-chain (1-157) containing C-terminal 8×His tag were also cloned into a pcDNA3.4 vector.

2.2 Protein expression and purification

Expi293F cells were cultured in Expi293 Expression medium (Gibco) in a 37 °C incubator with a humidified atmosphere of 8% CO_2 with shaking. Plasmids encoding the IgA1-Fc were transiently transfected into Expi293F or GnT-I(-) cells using ExpiFectamine 293 Transfection reagent and enhancer (Gibco). In the case of ^{13}C-labeling of the *N*-glycan, the cells were cultured in a medium containing [$^{13}C_6$] D-glucose (CIL). Transfection was carried out using Gxpress 293 Transfection & Medium Kit (Gmep, Japan) according to the manufacturer's instructions. Seven days following transfection, the supernatant was collected by centrifugation at $2{,}000 \times g$ for 30 min and applied to a column packed with anti-FLAG beads resin. The column was washed with phosphate-buffered saline (PBS), and the bound proteins were eluted with PBS containing 3×FLAG peptide (150 μg/mL). Eluted protein fractions were repeatedly concentrated and diluted with PBS with a 30-kDa MWCO Amicon centrifugal filter (Millipore, Ireland) to remove 3×FLAG peptide. The protein was checked by SDS-PAGE, with polyacrylamide at 12.5% or 5-20%. Briefly, samples were mixed with reducing loading buffer (10 mM DTT) and non-reducing (without DTT) conditions and heated in a metal bath for 5 min. Heated samples were subjected to electrophoresis in

polyacrylamide slab gels, after which gel staining was done with Coomassie Brilliant Blue (CBB) for 1 h.

For co-expression of IgA1-Fc and J-chain, the plasmid encoding the IgA1-Fc was transiently co-transfected with the plasmid encoding the J-chain into 30 mL Expi293F cells (3×10^6 cells/mL) with ExpiFectamine 293 Transfection Kit, using a total of 30 μg of DNA with varying ratios of IgA1-Fc and J-chain plasmids. Seven days following transfection, the supernatant was collected and the protein was purified using anti-FLAG resin as described above.

2.3 Trypsin digestion and reverse phase-HPLC separation

IgA1-Fc was dissolved at a concentration of 0.5 mg/mL in 500 mM Tris-HCl pH 8.0 containing 8 M Urea and incubated with 5 mg/mL DTT at 37℃ for 90 min, followed by alkylation with 40 mg/mL of iodoacetamide for 30 min. Then the solution was dialyzed against 20 mM ammonium bicarbonate pH 7.6. The sample was digested with MonoSpin Trypsin (GL Sciences) according to the manufacturer's instructions.

The reaction mixture was lyophilized and dissolved in 0.1%(v/v) TFA and loaded onto a C18 reverse-phase column (COSMOSIL 5C_{18}-AR, 4.6×250 mm, Nacalai Tesque, Japan) connected to an HPLC system (SCL-10Avp, Shimadzu, Japan) with mobile phase A: 0.1%(v/v) trifluoroacetic acid (TFA)/water, and B: 0.1%(v/v) TFA/water containing 90%(v/v) acetonitrile with a linear gradient of 0-90% acetonitrile in 0.1% TFA for 45 min. Absorbance was detected at 230 nm and 280 nm using UV-VIS detector SPD-10Avp (Shimadzu, Japan). The fractions collected per minute were lyophilized and then subjected to LC-MS and LC-MS/MS analysis.

2.4 LC-MS and LC-MS/MS analysis

LC-MS/MS analysis of the isolated peptides in reverse phase-HPLC was performed on an EASY-nLC 1200 HPLC connected to a Q Exactive mass spectrometer using a nanoelectrospray ion source (Thermo Fisher Scientific). The peptides were separated on a 75 μm inner diameter × 125 mm C18 reverse-phase column (Nikkyo Technos

NTCC-360) with a linear gradient from 0–35% acetonitrile with 0.1% formic acid for 0–30 min, followed by an increase to 95% acetonitrile during 35–45 min. The mass spectrometer was operated in data-dependent acquisition mode with a top 10 MS/MS method. MS1 spectra were measured with a resolution of 70,000, an AGC target of $3e^6$, and a mass range from 380 to 4,000 *m*/*z*. Higher-energy C-trap dissociation (HCD) [32] MS/MS spectra were acquired at a resolution of 17,500, an AGC target of $5e^5$, an isolation window of 1.6 *m*/*z*, a maximum injection time of 150 ms, and a normalized collision energy of 27. Dynamic exclusion was set to 15 s. LC-MS (full MS) analysis was also performed under the same condition to read the intensity of each ion peak.

The raw LC-MS/MS data obtained from the Q Exactive mass spectrometer were analyzed using Proteome Discoverer version 2.4 SP1 software made by Thermo Fisher Scientific. The software identified and quantified the peptides in the raw data by searching the UniProt-SwissProt database (release 2023_03) restricted to *Homo sapiens*. The search parameters used in the analysis were as follows: trypsin was set as the enzyme allowing up to two missed cleavages; a precursor mass tolerance of 10 ppm and a fragment mass tolerance of 0.5 Da were used; carbamidomethylation of cysteine was set as a fixed modification, while protein methionine oxidation was set as a variable modification.

Identification and quantification of glycopeptides were performed using Byonic™ (Protein Metrics) [33]. Peptides were filtered based on a false-discovery rate (FDR) of 1%, which means that the probability of a peptide being a false positive identification was less than 1%. Byonic's Glycopeptide Search was applied to the MS/MS data to identify glycopeptides in reference to the internal table of *N*-linked glycans. The Symbol Nomenclature for Glycans (SNFG) was used for the display of glycans [34].

2.5 Thermofluor assay

Thermal stability of IgA1-Fc and Fc-J-chain complexes was examined by fluorescence-based assay as previously described [35]. Briefly, the purified proteins were diluted in PBS to obtain the desired concentration (0.1 mg/mL) per well and 10

μL placed into PCR tubes strips, then 2.5 μL 50-fold diluted SYPRO Orange Dye (Invitrogen) was added to make up to a total volume of 12.5 μL. Following addition of the protein and the Orange Dye, the PCR tubes strips were sealed with an optical seal, mixed and centrifuged. The wavelengths for excitation and emission were 475–500 and 520–550 nm, respectively. Thermal scanning (20-95 ℃ at 8 ℃/min) was performed using a real-time PCR setup (PikoReal24, Thermo Scientific), and fluorescence intensity was measured every 4 s. The stability curve and its midpoint value (melting temperature, T_m) were obtained by gradually increasing the temperature to unfold the protein and measuring the fluorescence at each point.

2.6 ANS fluorescence assay

8-anilino-1-naphthalenesulfonic acid (ANS) was added to a final concentration of 140 μM into 0.3 mg/mL protein solution dissolved in PBS (pH 7.4). Then the samples were incubated at 37 ℃ in a black 96-microwell plate for 1 h. Fluorescence spectra were recorded every 2 nm wavelength using a SpectraMax iD5 multi-mode microplate reader (Molecular Devices, USA) at an excitation wavelength of 367 nm, and emission wavelength from 407 to 607 nm.

2.7 Western blotting and Lectin blotting

Equal amounts of purified proteins were applied to non-reducing SDS-PAGE. After electrophoresis, the proteins were transferred to a PVDF membrane (Millipore, USA) and then blocked with 5% BSA for 1 h. The blocked membrane was incubated with a 1:3000 dilution of anti-FLAG-HRP or anti-Histidine-tag-HRP antibodies overnight at 4 ℃. The immunoreactive bands were detected using an Immobilon® Forte Western HRP Substrate (Millipore, USA) according to the manufacturer's instructions.

For lectin blotting, the membrane was incubated overnight with a 1:3000 dilution of a series of biotinylated lectins (COSMO Bio Co., LTD), concanavalin A (ConA), *Phaseolus vulgaris* leucoagglutinin (PHA-L4), *Phaseolus vulgaris* erythroagglutinin (PHA-E4), *Maackia amurensis* (MAM), *Sambucus sieboldiana* (SSA) and *Aleuria*

aurantia lectin (AAL). Vectastain ABC kit (Vector Laboratories, Burlingame, CA, USA) was used to bind both avidin and biotinylated-conjugated HRP. The immunoreactive bands were also detected using an Immobilon® Forte Western HRP Substrate according to the manufacturer's instructions. The molecular weight was indicated using YesBlot^{TM} Western Marker I (SMOBiO).

2.8 Size exclusion chromatography

Proteins were further analyzed using an HPLC system (Hitachi). Based on the molecular weights and the multimeric states of the proteins, Superdex 200 pg column (Cytiva) was used for assessment of the multimeric state for IgA1-Fc and testing the complex formation. The column was equilibrated with PBS (pH 7.4) at a flow speed of 0.5 mL/min, after which 100 μL of protein sample was injected into the HPLC system. Fractions were collected at one-minute intervals and the protein detected by Western blotting. The elution volume was calibrated using a low molecular weight gel filtration marker kit from 6,500 to 200,000 Da (Cytiva). Elution times of standard proteins were as follows: 28.3 min for ovalbumin (44 k), 26.3 min for conalbumin (75 k), 24.5 min for aldolase (158 k), 18.2 min for ferritin (440 k), and 16.8 min for thyroglobulin (669 k). Blue Dextran 2000 (2,000 k) was also applied to estimate the void volume of the column (7.9 mL, eluted at 15.8 min).

2.9 NMR spectroscopy

All NMR experiments were recorded on an 800 MHz spectrometer equipped with a cryogenic triple resonance probe (Bruker). The probe temperature was set at 308 K. The Fc sample was dissolved in 20 mM sodium phosphate (pH 7.4) containing 100 mM NaCl in D_2O (D: 99.96%). 2D ^{1}H-^{13}C heteronuclear multiple quantum coherence (HMQC) spectra were recorded with 128 scans. ^{1}H and ^{13}C chemical shifts are given in ppm calibrated with internal reference DSS (4,4-dimethyl-4-silapentane-1-sulfonic acid) at 0 ppm. Spectral measurement, data processing and spectral display were performed using TopSpin Version 4 (Bruker).

2.10 Model building of *N*-glycosylated Fc-J-chain complex

Glycan Modeler tool in CHARMM-GUI [36] was used to build a 3D structural model of *N*-glycosylated Fc-J-chain complex. A cryo-EM structure of dimeric sIgA-Fc complex (PDB ID: 6UE7) was used as a scaffold. N263 and N459 of Fc and N49 of J-chain were modeled to form the core $Man_3GlcNAc_2$ structure. When the inner core of the *N*-glycan was observed, the glycan was extended using the coordinates from Glycan Fragment Database [37]. When the glycan is entirely missing, the $Man_3GlcNAc_2$ glycan was added based on the CHARMM force field [38].

3. Results and Discussion

3.1 IgA1-Fc predominantly exists as a monomer in solution

To evaluate the role of individual *N*-glycans in IgA1, we designed four IgA1-Fc constructs in which Cys471 interacting with the J-chain was mutated to Ser and the glycosylation sites were mutated to Gln individually or collectively (Fig. 2A, 2B). This N-to-Q mutation is appropriate for evaluating the role of *N*-glycan in a site-specific manner; however, the results need to be interpreted carefully as the substitution itself, even though conservative, may have an effect. We also assumed that the glycosylation status of the remaining sites in mutants is similar to the corresponding glycan in wild-type molecule. We used a truncated IgA1-Fc instead of an intact IgA1 molecule, because IgA1-Fc is sufficient to form a dimer with the J-chain [5] and the solution NMR analysis is simpler owing to its smaller size. The plasmids were transfected into mammalian Expi293F cells to transiently express recombinant IgA1-Fc. After purification of recombinant FLAG-tagged IgA1-Fc, we first characterized the four constructs with SDS-PAGE under reducing and non-reducing conditions (Fig. 2C). IgA-Fc (C471S) showed a broad band at ~30-35 kDa under the reducing condition and at ~65 kDa under the non-reducing condition. Doubling of the estimated molecular mass under the non-reducing condition suggests that the inter-chain disulfide bonds at the hinge region formed correctly to shape the Fc molecule. The estimated molecular mass under the reducing condition (~30-35 kDa) was slightly higher than the theoretical molecular mass (27 kDa), suggesting the modification of heterogeneous *N*-glycans in Fc. This was evidenced by the differences in migration for three *N*-glycosylation mutants, C471S/N263Q, C471S/N459Q, and C471S/N263Q/N459Q. The step-wise increase in mobility suggests that N263 and N459 are both *N*-glycosylated. It has been reported that *N*-linked oligosaccharides contribute considerably to the total mass of IgA [39]. The migrations differ between C471S/N263Q and C471S/N459Q, suggesting that different types of *N*-glycans attach to each *N*-glycosylation site. In addition, these three mutants showed molecular masses of ~50 kDa under the non-reducing condition, showing that inter-chain disulfide bridges can be formed regardless of the *N*-

glycosylation at both sites. Judging from the SDS-PAGE pattern, IgA1-Fc was successfully expressed and secreted as an Fc-monomer in the absence of J-chain.

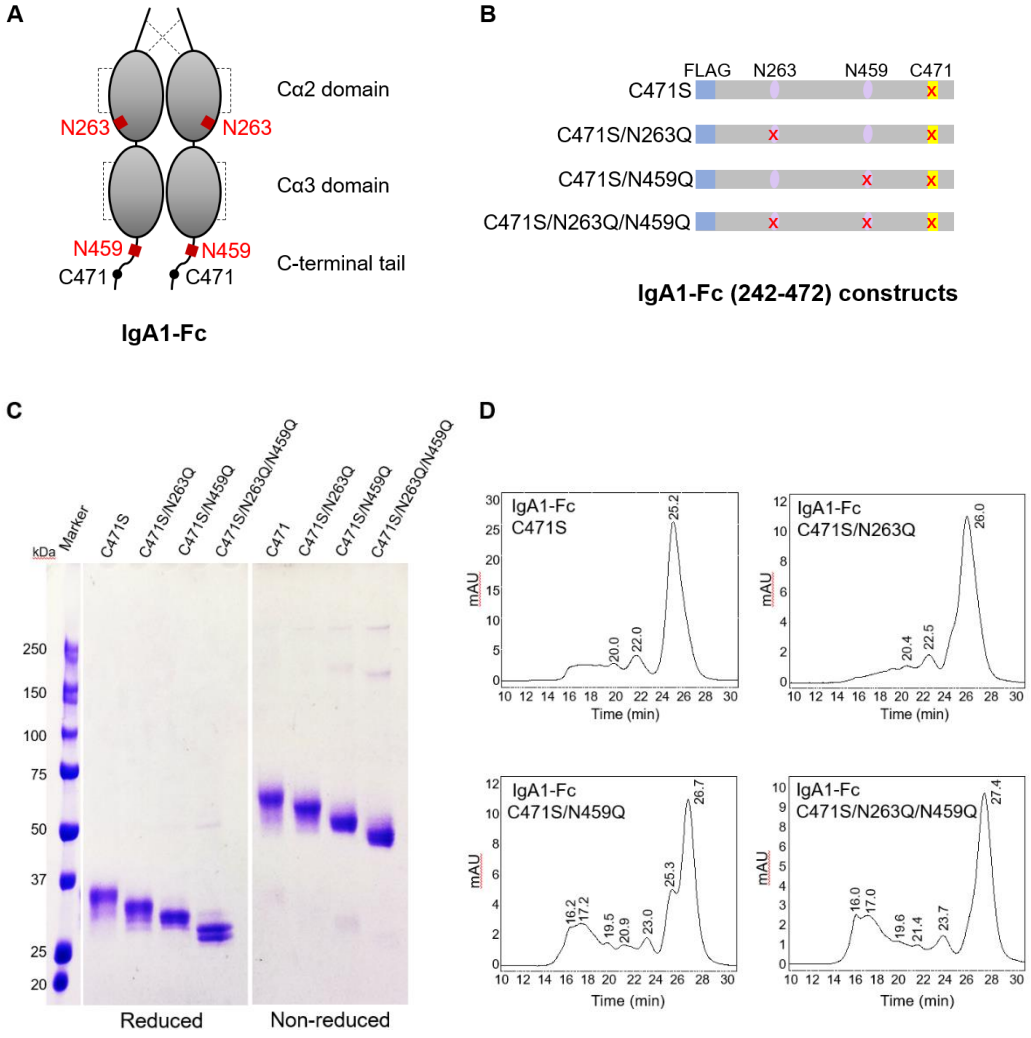

Figure 2. Recombinant expression of IgA1-Fc mutants in Expi293F cells.

(A) Schematic drawing of IgA1-Fc monomer with *N*-glycosylation sites (red squares), inter- and intra-chain disulfide bonds (dashed lines). (B) Constructs of IgA1-Fc (242-472) mutants (C471S, C471S/N263Q, C471S/N459Q and C471S/N263Q/N459Q) used in this study. (C) SDS-PAGE of IgA1-Fc mutants (C471S, C471S/N263Q, C471S/N459Q and C471S/N263Q/N459Q) purified from culture supernatant of Expi293F cells under reducing and non-reducing conditions. Protein bands were stained with CBB. (D) Size-exclusion chromatography of the affinity-purified IgA1-Fc mutants. The peaks were detected by absorbance at 280 nm (mAU). Flow rate of the mobile phase was set to 0.5 mL/min.

To examine the oligomeric state of IgA1-Fc in solution, the purified IgA1-Fc samples were applied to size exclusion chromatography (SEC) (Fig. 2D). C471S eluted at 25.2 min (12.6 mL) as a major peak, which corresponds to 95 kDa as calculated from the elution volumes of standard proteins. The three other mutants (C471S/N263Q, C471S/N459Q, and C471S/N263Q/N459Q) also showed a major peak at 26.0 min (13.0 mL), 26.7 min (13.4 mL) and 27.4 min (13.7 mL), corresponding to molecular masses of 83 kDa, 69 kDa and 57 kDa, respectively. These retention times (elution volumes) are slightly larger than that of C471S, possibly due to the complete or partial loss of *N*-glycans in these mutants. The estimated molecular mass of 57 kDa for C471S/N263Q/N459Q suggests a monomer in solution (54 kDa). The degree of *N*-glycosylation shows that the other mutants are also present as predominantly monomers. It should be noted that C471S/N459Q and C471S/N263Q/N459Q showed several additional broad peaks at 16-18 min, suggesting that C471S/N459Q and C471S/N263Q/N459Q partially formed higher oligomers. It appears that N459 glycans influence the multimerization of IgA1-Fc.

3.2 *N*-glycans of IgA1-Fc are site-specifically modified

To investigate the type of *N*-glycans attached to IgA1-Fc, lectin blotting was performed using ConA, PHA-L4, PHA-E4, MAM, SSA and AAL (Fig. 3). The amounts of IgA1-Fc detected by anti-FLAG antibody were confirmed to be the same as those stained with CBB, and the molecular mass is about 30 kDa under the reducing condition. Comparing the patterns of four mutants (C471S, C471S/N263Q, C471S/N459Q, C471S/N263Q/N459Q), it was found that the C471S/N263Q/N459Q mutant was not stained by any lectins tested and N263 and N459 are site-specifically modified with *N*-glycans. A clear example is AAL-lectin blotting, showing that the N459-glycan contains α-linked fucose, but the N263-glycan does not. MAM and SSA lectin staining data suggest the presence of α2-3Sia in N459-glycan and α2-6Sia in both N263- and N459-glycans. It should be noted that C471S/N263Q showed a broad band as detected by anti-FLAG antibody, which may be correlated with the heterogeneity of *N*-glycan

attached onto N459.

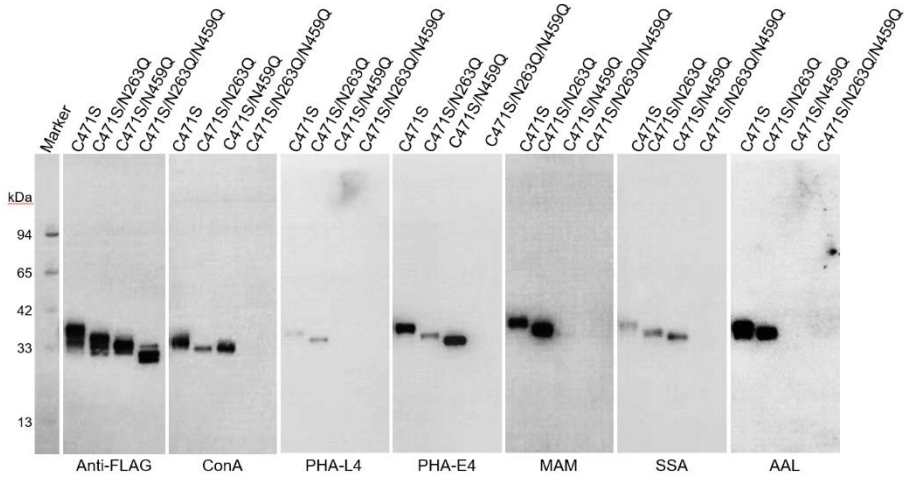

Figure 3. Typing of N-glycans attached to recombinant IgA1-Fc mutants.

Lectin blotting of IgA1-Fc mutants (C471S, C471S/N263Q, C471S/N459Q and C471S/N263Q/N459Q) using ConA, PHA-L4, PHA-E4, MAM, SSA and AAL. The membrane was incubated with anti-FLAG antibody-HPR to show the position of IgA1- Fc (left).

To more conclusively investigate the composition of *N*-glycans attached to IgA1-Fc, purified proteins were treated with trypsin and the resulting peptide mixtures were subjected to reverse-phase HPLC and mass spectrometry analyses. To identify the glycopeptide fractions, we compared the HPLC patterns of peptide mixtures from three different IgA1-Fc proteins (C471S, C471S/N263Q and C471S/N459Q) (Fig. 4). Some

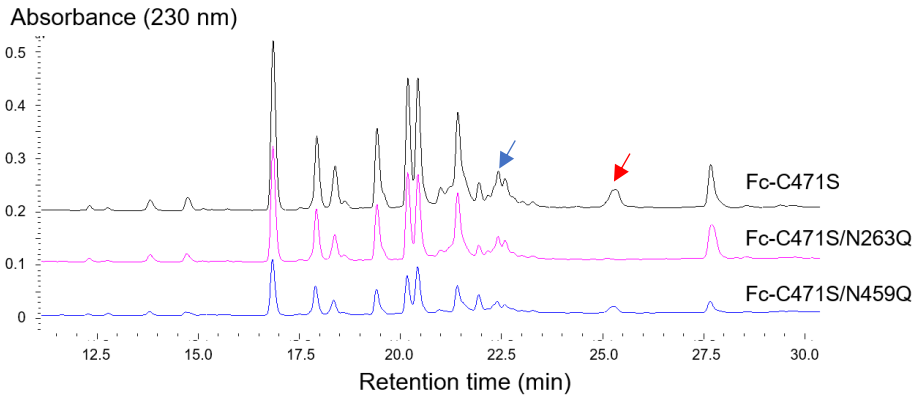

Figure 4. Identification of glycopeptides by comparing RP-HPLC patterns.

C471S, C471S/N263Q and C471S/N459Q were treated by trypsin and then subjected to RP-HPLC. N263-glycopeptide and N459-glycopeptied were indicated by blue and red arrows respectively.

selected fractions from C471S were subjected to LC-MS and LC-MS/MS analysis and peaks eluted at 22-23 min and 25-26 min were identified as the glycopeptide [L246-R272] containing N263 and [L451-Y472] and as that containing N459, respectively (Fig. 5A, B). The other fractions did not contain the glycopeptides.

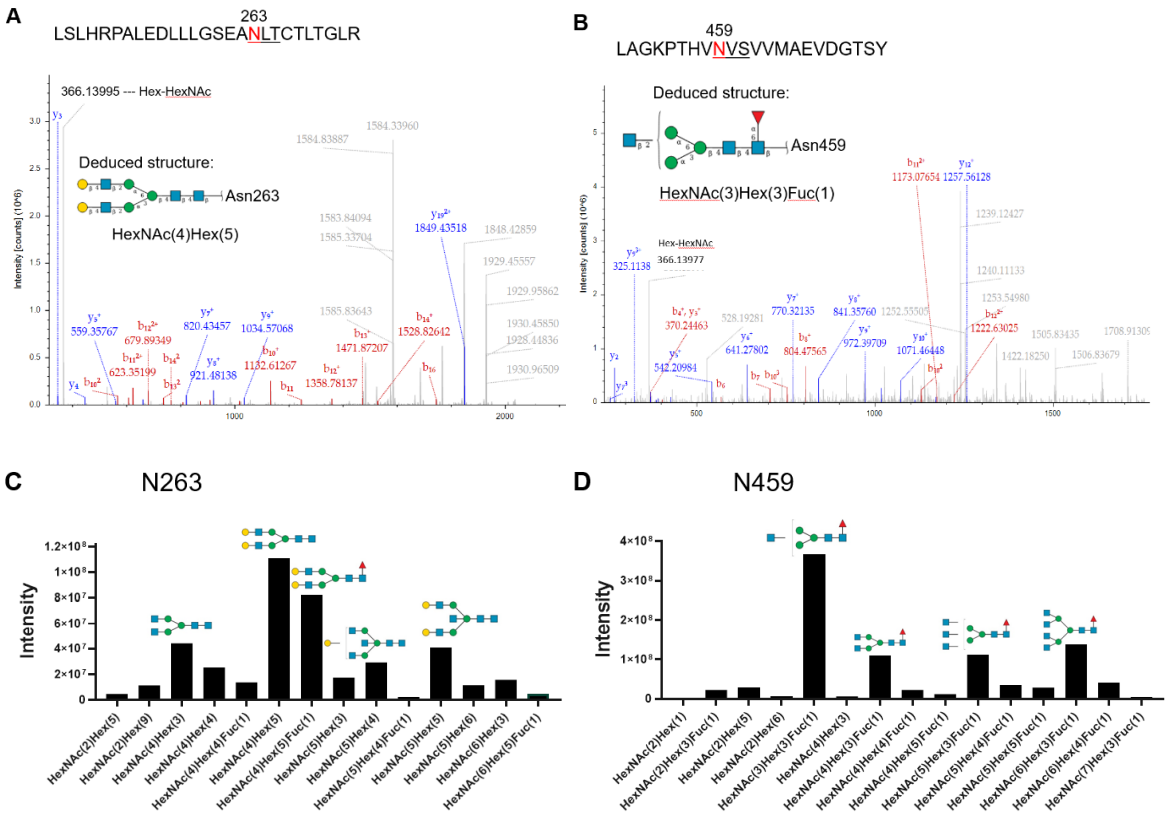

Figure 5. Mass spectrometry analysis of *N*-glycans attached to recombinant IgA1-Fc mutants.

(A, B) Composition of *N*-glycan attached onto N263 (B) and N459 (C). Determination of glycan composition was performed using Byonic software. The intensity of each ion peak was read from LC-MS and displayed in the graph, whose Byonic scores were more than 200 for N263-containing peptides, and 300 for N459-containing peptides. For peaks of high intensity, deduced structure(s) are shown on the top of each bar. The intensity was shown as the sum of the intensities from multiply charged peaks.

Diagnostic glycan fragment ions were detected for both glycopeptides; an oxonium ion with m/z = 366.14 (Hex-HexNAc) was detected for both glycopeptides, and a fragment

ion with m/z = 528.19 (Hex_2-HexNAc) was detected for the glycopeptide containing N459. Glycan structures were found to be heterogeneous for both sites and each composition was identified using Byonic software. To gain a rough estimate of the relative ratio of each glycan composition, we read the intensities of the parent ion in the LC-MS (full MS) spectrum. The results are summarized in Figures 5C and 5D. Although we could not uniquely determine the glycan structures solely from the MS data, the composition data can be used to discuss the *N*-glycan types: the *N*-glycan at N263 is mostly of the biantennary complex-type, fucose rarely appeared and galactose proved plentiful. Unglycosylated peptide [L246-R272] was not detected in the fraction eluted at 25-26 min. In contrast, the *N*-glycan at N459 is lacking galactose and mostly fucosylated. High mannose type glycans were found at both sites but the amount is very low. A small fraction of unglycosylated peptide [L451-Y472] was detected at the ion intensity of 9.2×10^6.

Taken together, both N263 and N459 are site-specifically modified, with distinct trimming/maturation procedures, suggesting that the environments of these asparagine residues are different. The MS data suggested that N263-glycan is galactose-terminated, and fucose is lacking (Fig. 5C). N459 is mostly fucosylated and galactose is lacking (Fig. 5D). These results are roughly consistent with lectin-blotting data (Fig. 3). The difference is that sialylated glycans were not significantly observed in the MS analysis. This may be due to a low degree of sialylation of IgA1-Fc glycans, because lectin blotting is qualitative. Another possible reason is that routine mass analysis of sialylated glycans and glycoconjugates is often affected by the loss of sialic acid residues that occurs during post ionization [40, 41].

These results can be compared with previous reports analyzing the *N*-glycan structure of IgA1 site-specifically [14]. Tanaka et al. examined IgA1 from normal human serum and reported that N263 was mainly modified with fully galactosylated biantennary glycan while N459 attached fully fucosylated biantennary glycan [42]. Mattu et al. analyzed recombinant human IgA1 from CHO cells. N263 contained mostly biantennary glycans while N459 contained mostly triantennary glycans [43]. Goritzer

et al. reported the site-specific *N*-glycosylation of recombinant human IgA1 from HEK293 cells. N263 was predominantly modified with biantennary unfucosylated glycan while N459 mainly contained core-fucosylated and multibranched structures [44]. Although the human IgA1 sources were different (serum or recombinant), the results, overall, indicate the presence of non-fucosylated biantennary glycan at N263 and more branched, fucosylated glycan at N459.

3.3 Effect of each *N*-glycan on the stability of IgA1-Fc

To investigate the role of *N*-glycans, we prepared a series of *N*-glycosylation mutants. A thermofluor assay was first performed to determine the melting temperature (T_m) using these samples (Fig. 6A). IgA1-Fc C471S and C471S/N459Q showed similar T_m (70.3 and 70.5 ℃), suggesting that N459-glycan at the C-terminal tail did not significantly contribute to the thermal stability. In contrast, a significant decrease in T_m was observed for IgA1-Fc C471S/N263Q (66.0 ℃) and C471S/N263Q/N459Q (66.3 ℃). The results indicate that N263-glycan contributes to the stabilization of IgA1-Fc. In C471S/N459Q and C471S/N263Q/N459Q, we noticed a slightly higher fluorescence intensity at 20 ℃. This would tie in with an exposed hydrophobic region around the C-terminal tail due to loss of the *N*-glycan cover at N459.

We then used a hydrophobic fluorescent probe, 8-anilino-1-naphthalenesulfonic acid (ANS) [45], to directly report on the hydrophobic surface of IgA1-Fc (Fig. 6B). C471S/N459Q and C471S/N263Q/N459Q showed slightly higher fluorescence intensity compared with C471S and C471S/N263Q. This again indicates a more hydrophobic surface in the N459Q mutants, which may correlate with the observation that N459Q mutants contain only a small fraction of oligomeric species as detected in size-exclusion chromatography (Fig. 2D). These results suggest that the N263-glycan stabilizes Fc, while the N459-glycan covers a hydrophobic surface at the C-terminal tailpieces.

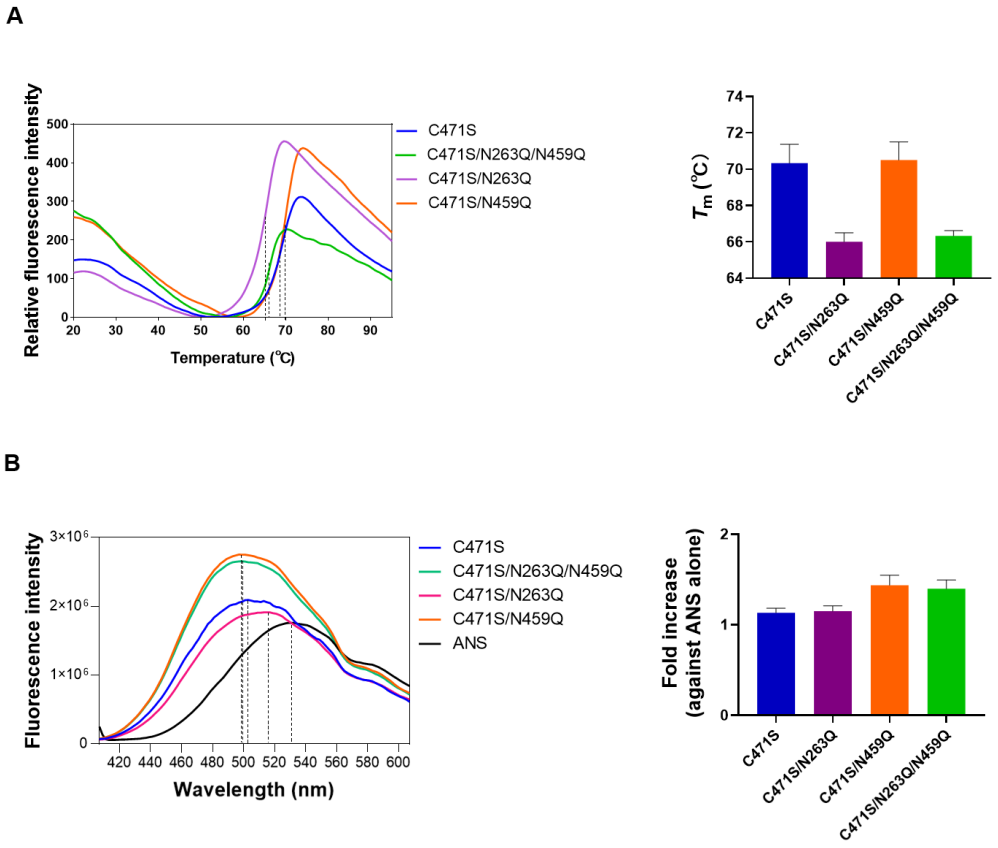

Figure 6. Analysis of thermal stability and surface hydrophobicity of IgA1-Fc mutants using fluorescent probes.

(A) T_m measurement of IgA1-Fc mutants by thermofluor assay using SYPRO Orange. Excitation and emission wavelengths were 475-500 and 520-550 nm, respectively. Bar graph on the right shows T_m of each mutant. The average T_m values are indicated with standard deviation from three independent experiments (n = 3). (B) Analysis of surface hydrophobicity using the fluorescent probe ANS. Fluorescence spectra of ANS were recorded in the presence or absence of Fc. Excitation wavelength was set to 367 nm, and emission spectra were recorded from 407 nm to 607 nm. Bar graph on the right shows the fold increase of the maximum ANS fluorescence intensity in the presence of each mutant compared with that of ANS without protein.

Next, we examined whether glycan composition affects the thermal stability and surface hydrophobicity. For this purpose, we produced IgA1-Fc proteins with homogeneous $Man_5GlcNAc_2$ glycan using an Expi293F GnT-I(-) cell line which lacks

N-acetylglucosaminyltransferase I (GnT-I) activity. The recombinant IgA1-Fcs (C471S, C471S/N263Q and C471S/N459Q) obtained using the Expi293F GnT-I(-) cells (designated as C471S/N263Q-Man5, C471S/N459Q-Man5) were first analyzed by SDS-PAGE under reducing and non-reducing conditions (Fig. 7A).

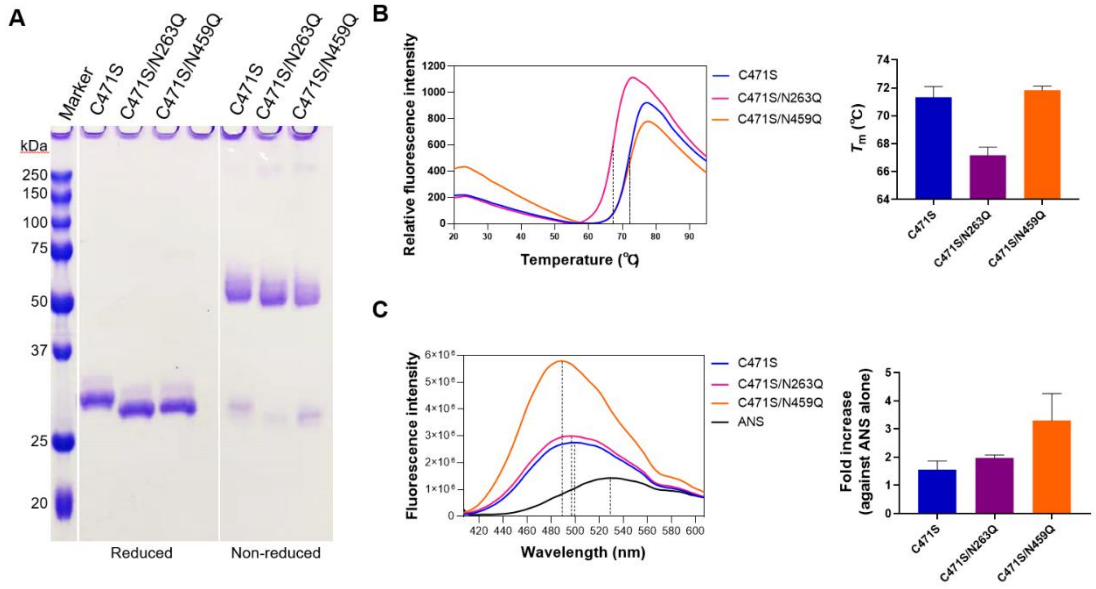

Figure 7. Recombinant expression of IgA1-Fc using Expi293F GnT-I(-) cells.

(A) SDS-PAGE of IgA1-Fc purified from the culture supernatant of Expi293F GnT-I(-) cells under reducing and non-reducing conditions. (B) The melting temperature (T_m) of IgA1-Fc from Expi293F GnT-I(-) cells was obtained from the midpoint value of the stability curve (fluorescence intensity and real time). The average Tm values are indicated with standard deviation from three independent experiments (n = 3). (C) Surface hydrophobicity of IgA1-Fc from Expi293F GnT-I(-) cells assessed using ANS fluorescence. Fluorescence spectra of ANS were recorded at 367 nm excitation wavelength, and 407 nm-607 nm emission wavelength.

Compared with Expi293F cells, IgA1-Fcs from Expi293F GnT-I(-) cells showed sharper bands and the migrations were slightly larger under the reducing condition. Under the non-reducing condition, IgA-Fcs (Man5) migrated as 57 kDa, this being twice that found in the reducing condition (27 kDa). T_m was also measured to determine the thermal stability of IgA1-Fc expressed in Expi293F GnT-I(-) cells (Fig. 7B). C471S/N263Q-Man5 showed lower T_m than C471S-Man5 and C471S/N459Q-Man5,

suggesting that glycan composition does not significantly affect the T_m. The denaturation temperatures of IgA1-Fc (Man5) from Expi293F GnT-I(-) cells are slightly higher than those of IgA1-Fc from Expi293F cells, implying that the terminal modifications of complex-type glycans slightly affect the stability of Fc. Higher fluorescence intensity was also observed for C471S/N459Q-Man5 from Expi293F GnT-I(-) cells at 20°C (Fig. 7B), as seen in IgA1-Fc C471S/N459Q from Expi293F cells (Fig. 6A). The ANS fluorescence assay also suggested the exposure of a hydrophobic surface in C471S/N459Q-Man5 (Fig. 7C). These trends concur with the data obtained using Fc from Expi293F cells. Modification of N263 and N459 with homogeneous $Man_5GlcNAc_2$ glycan is therefore sufficient to stabilize Fc and cover the hydrophobic surface, and further terminal modifications have limited structural consequences.

3.4 Dynamics of IgA-Fc *N*-glycans assessed by ^{13}C-assisted NMR

To further clarify the structural and functional role of each *N*-glycan, we performed NMR analysis of IgA1-Fc with the aid of ^{13}C-labeling, as performed in IgG-Fc analyses [46-48]. IgA1-Fc (C471S), was expressed in a medium containing [$^{13}C_6$] D-glucose to incorporate ^{13}C into the *N*-glycans. Purified IgA1-Fc (C471S) was subjected to 2D ^{1}H-^{13}C HMQC measurement (Fig. 8A). We observed characteristic signals in the carbohydrate area (^{13}C 95-105 ppm for anomeric signals and 60-80 ppm for non-anomeric signals), suggesting that the ^{13}C enrichment into the *N*-glycans attached onto IgA1-Fc was successful. Significantly, we could uniquely identify a GlcNAc-1 C1-H1 correlation signal (^{13}C ~80 ppm/^{1}H ~5 ppm). To assign the carbohydrate signals in a site-specific manner, we prepared ^{13}C-labeled mutants C471S/N263Q and C471S/N459Q. A comparison of the three appropriate NMR spectra showed that that of C471S/N263Q is similar to that of C471S, while the signals of C471S/N459Q are significantly weaker (Fig. 8A). We extracted the ^{13}C slices at 80 ppm which includes the GlcNAc-1 anomeric signal (^{1}H 5 ppm). C471S and C471S/N263Q showed a strong sharp signal, while that of C471S/N459Q was extremely weak (Fig. 8B). Broadening

of NMR signals reflects limited mobility or the presence of chemical exchange.

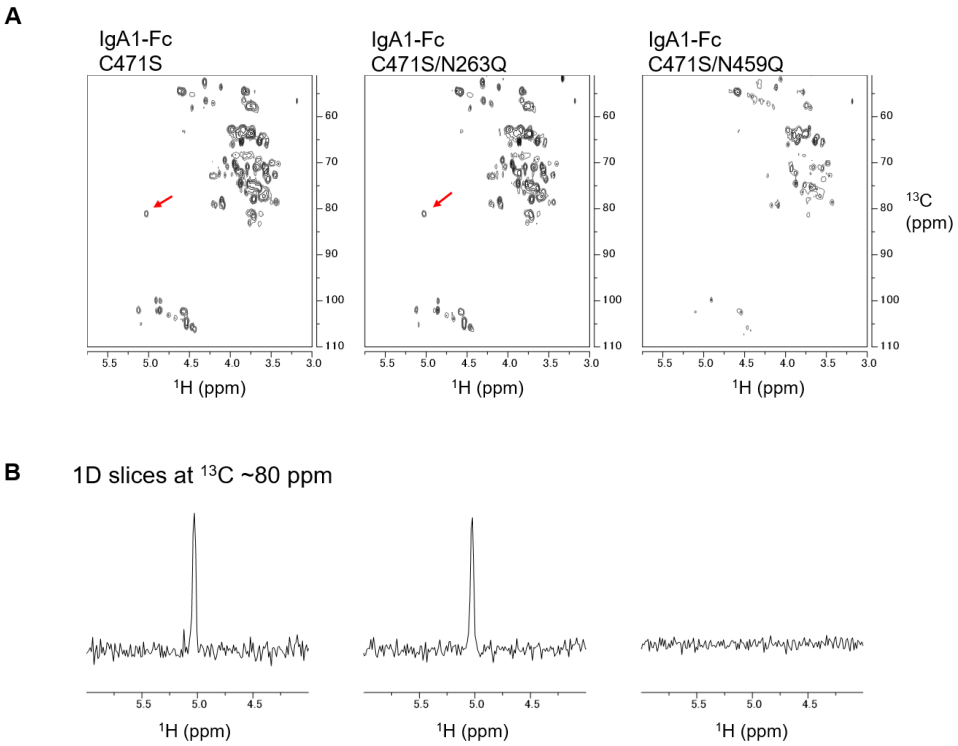

Figure 8. NMR analysis of the glycan dynamics using ^{13}C-labeled IgA1-Fc mutants.

(A) 2D ^{1}H-^{13}C HMQC spectra of ^{13}C-labeled IgA-Fc mutants (C471S, C471S/N263Q and C471S/N459Q) at ^{1}H observation frequency of 800 MHz. (B) 1D slices (at ^{13}C 80 ppm) were extracted from ^{1}H-^{13}C HMQC spectra, which correspond to anomeric carbon C1 of the *N*-linked GlcNAc residue.

In C471S/N459Q, the other anomeric signals (^{13}C ~100 ppm) and non-anomeric signals were weak but significant. This observation supports the notion that the broadening of the GlcNAc-1 anomeric signal in C471S/N459Q is due to the limited mobility, rather than originating from chemical exchange effects. The sharp signal from the N459-glycan at the C-terminus likely reflects an extremely flexible moiety, while the weak one from the N263-glycan suggests immobilization. The latter observation suggests extensive interaction between the N263-glycan and the Fc polypeptide, which supports the thermofluor assay data. Although the location of N263 in IgA1-Fc is different from that of N297 in IgG-Fc, the structural role of *N*-glycan seems similar. It is of note then that stabilization of Fc by *N*-glycosylation is not limited to the modification at N297 in

IgG-Fc and therefore each immunoglobulin class and subclass needs to be analyzed in order to elucidate the individual role of *N*-glycosylation. A further point is that the flexibility of N459-glycans may correlate with suppression of higher-order polymers at the C-terminal tail.

3.5 IgA1-Fc formed a dimer in the presence of J-chain

The assembly of polymeric IgA requires co-expression of J-chain and IgA1-Fc. To produce the Fc dimer recombinantly, we tried to maximize dimer formation by changing the ratio of J-chain DNA and IgA1-Fc DNA. Co-expression of IgA1-Fc WT with J-chain WT at a DNA ratio of 1:4 resulted in a reasonable yield, mainly of secreted IgA1-Fc dimer and some tetramer (data not shown). We used this DNA ratio in our subsequent studies of expressed Fc-J-chain complex.

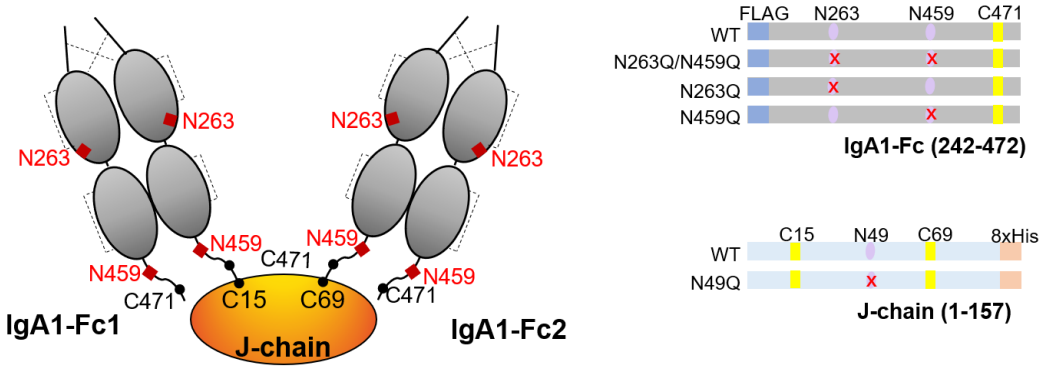

Figure 9. Schematic drawing of IgA1-Fc dimer and constructs designing.

(A) Schematic drawing of IgA1-Fc dimer in complex with J-chain. *N*-glycosylation sites (red squares) and inter-chain disulfide bonds (dashed lines) are shown. (B) Constructs of IgA1-Fc (wild-type, N263Q, N459Q and N263Q/N459Q) and of J-chain (wild-type and N49Q).

To determine the role of *N*-glycans on IgA1 polymerization, mutations at *N*-glycosylation sites (N49Q in J-chain, N263Q and/or N459Q in IgA1-Fc) were introduced, as shown in Fig. 9A, B. The Fc complexes were purified using anti-FLAG antibody beads and checked by SDS-PAGE under reducing and non-reducing conditions. Under the reducing condition, IgA1-Fc appeared at 30 kDa, and the J-chain at 22 kDa, which is somewhat larger than the theoretical molecular mass (17 kDa) (Fig.

10A). Under the non-reducing condition, there is a major band at ~150 kDa and a minor band at 300 kDa for the complex of J-chain WT and IgA1-Fc WT. The observed masses are slightly higher than those of the theoretical dimeric (125 kDa) and tetrameric (233 kDa) Fc with J-chain. Monomeric Fc was not detected, suggesting that J-chain significantly contributes to the formation of Fc dimer and tetramer under this condition. When the two *N*-glycosylation sites (N263 and N459) of Fc were both mutated, the bands appeared at ~130 kDa and ~260 kDa, corresponding to dimeric and tetrameric IgA1-Fc in the presence of J-chain. Each of the *N*-glycosylation mutants (N263Q or N459Q) showed similar bands at positions slightly above 130 kDa and 260 kDa due to the presence of *N*-glycans. These observations suggest that wild-type and the glycosylation mutants can form dimeric IgA1-Fc in the presence of J-chain. It should be noted, however, that N459Q and N263Q/N459Q mutants without *N*-glycan at the tailpiece of IgA1 showed a smeared broad band above 260 kDa, and the relative amount of dimeric IgA1-Fc was significantly decreased compared with wild-type Fc and the N263Q mutant. These results suggest that N459Q and N263Q/N459Q mutants were produced to include higher-order polymers, while the N263 mutant appeared mainly as a dimer like wild-type Fc (Fig. 10A). It is likely that *N*-glycosylation at N459 prevents the formation of abnormal higher-order polymers.

To examine the role of *N*-glycosylation at N49, we expressed wild-type IgA1-Fc in the presence of J-chain mutant N49Q. Expression revealed mainly dimer but also some tetramer. The data suggest that the *N*-glycan at J-chain N49 is not essential for the coupling of IgA1-Fc with J-chain. This contradicts a previous study [30]. Possible reasons are: Firstly, Krugmann et al expressed the complex using mouse J-chain which differs slightly from human J-chain; secondly, the previous study explored the role of N49-glycans of the J-chain with intact heavy chain and light chain. In our experiment, however, Fc fragment and J-chain were used without light chain; thirdly, the extent of complex formation may be different in different cell lines.

Western blotting using anti-FLAG and anti-histidine tag antibodies certified that all the oligomers contained both J-chain and Fc (Fig. 10B). Also, we tried to express J-chain alone in the absence Fc. Purified proteins were found to be mostly oligomers/multimers, without distinctive smaller structural entities (data not shown), consistent with previous reports [15, 21, 29].

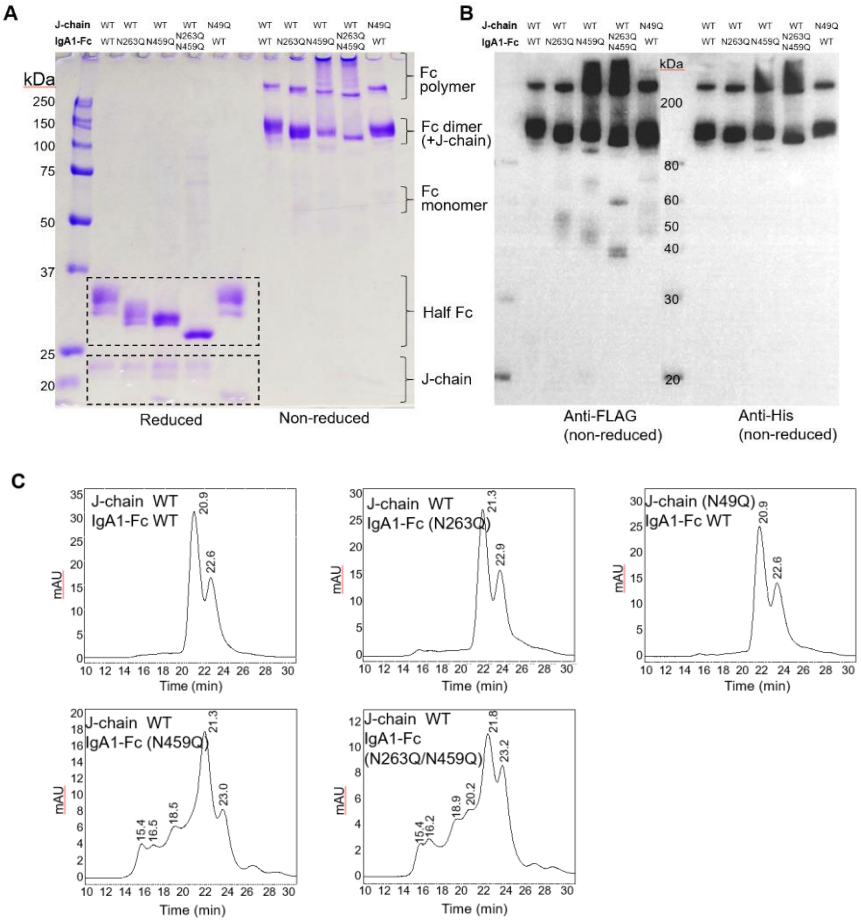

Figure 10. Oligomerization of IgA-Fc is affected by *N*-glycans attached to Fc tailpiece.

(A) SDS-PAGE of the expressed and purified proteins using combinations of IgA1-Fc and J-chain plasmids. The bands were stained with CBB under reducing and non-reducing conditions. Bands of Fc monomer, dimer and polymer are indicated according to different molecular sizes. Bands from reduced Fc (half Fc) and J-chain are boxed with dotted line. (B) The SDS-PAGE gel under non-reducing condition was applied for Western blotting with anti-FLAG (detecting IgA1-Fc) or anti-His-tag (J-chain) antibodies. (C) Size-exclusion chromatography analyses of affinity-purified IgA1-Fc-J-chain complexes. The protein peaks were detected by absorbance at 280 nm (mAU).

The Fc-J-chain complexes were also subjected to SEC to further examine the oligomeric states in solution (Fig. 10C). There are two peaks with the J-chain WT and IgA1-Fc WT complex at 22.6 min (11.3 mL) and 20.9 min (10.5 mL), corresponding to 180 and 260 kDa. The predominant peaks of J-chain WT and IgA1-Fc (N263Q/N459Q) complex are found at 23.2 min (150 kDa) and 21.8 min (210 kDa). The two lower estimated molecular masses (180 and 150 kDa) are roughly consistent with the theoretical value for a dimeric IgA1-Fc with J-chain (130 kDa), and the discrepancy is possibly due to *N*-glycosylation differences. The estimated molecular mass of 210 kDa is roughly consistent with the theoretical molecular mass for tetrameric IgA1-Fc with J-chain (230 kDa). N459Q and N263Q/N459Q with wild-type J-chain showed characteristic elution patterns, with additional peaks at 14-20 min. This observation implies the formation of higher-order oligomers, consistent with the result of SDS-PAGE. N459-glycan evidently plays an essential role on the assembly of proper dimeric IgA.

3.6 Structure of *N*-glycans attached onto dimeric IgA1-Fc

To check the *N*-glycosylation pattern of Fc and J-chain, lectin blotting was performed (Fig. 11). The complexes of IgA1-Fc and J-chain were detected by anti- FLAG and anti-

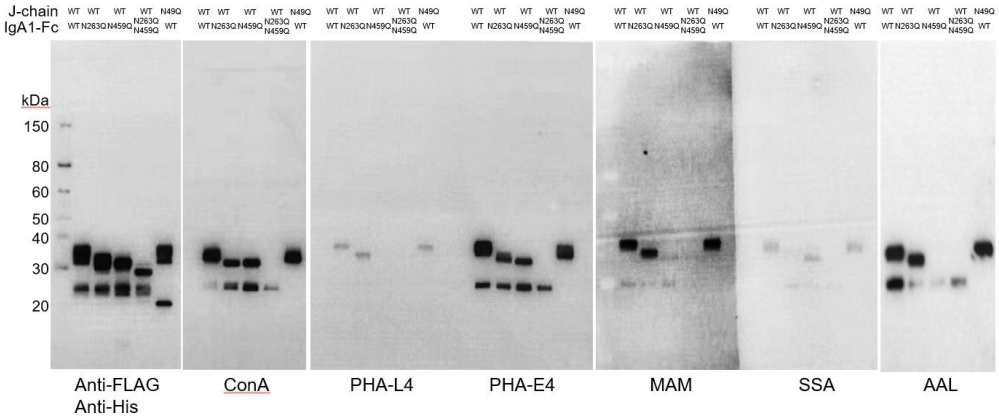

Figure 11. Typing of the N-glycans attached to IgA1-Fc and J-chain complexes. Lectin-blotting of IgA1-Fc-J-chain complexes using ConA, PHA-L4, PHA-E4, MAM, SSA and AAL. The membrane was incubated with anti-FLAG antibody-HPR and anti-histidine tag antibody-

HPR to show the position of IgA-Fc and J-chain (left).

histidine tag antibody with IgA1-Fc and J-chain at 30-35 kDa and 22 kDa, respectively under the reducing condition. ConA lectin blotting showed that N459Q attaches more high-mannose glycans than N263Q. IgA1-Fc and J-chain in the complexes contain bisecting GlcNAc residues in both Fc and J-chain as detected with PHA-E4 lectin. Lectin blotting using MAM and SSA revealed that almost all the sialic acids are attached as Siaα2-3Gal on N459. Blotting using AAL showed that fucose is present mainly at the N459-glycan.

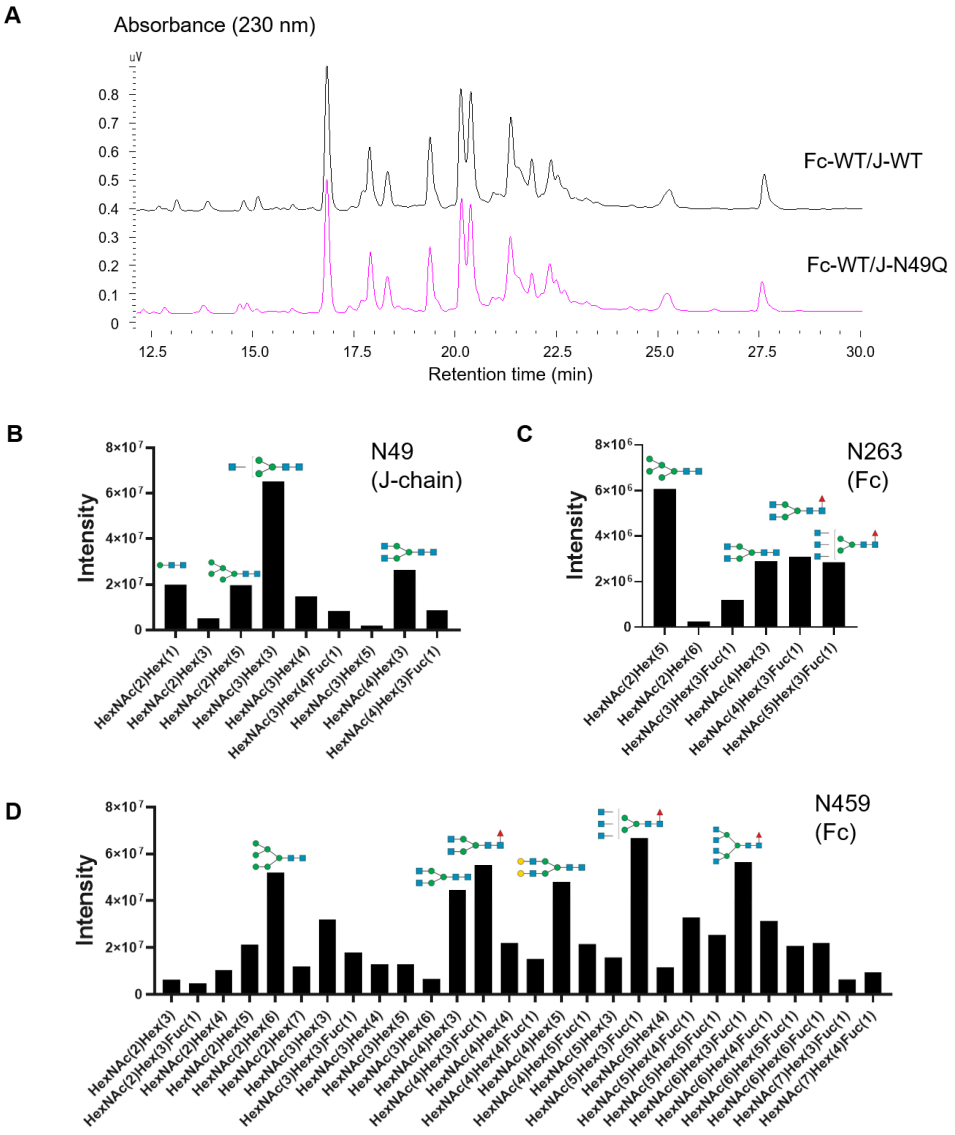

Figure 12. Mass spectrometry analysis of the *N*-glycans attached to IgA1-Fc and J-chain

complexes.

(A) RP-HPLC patterns of tryptic peptide mixtures from the IgA1-Fc and J-chain complexes (Fc-WT/J-chain WT and Fc-WT/J-chain N49Q). (B, C, D) Composition of *N*-glycan attached onto J-chain N49 (B), Fc N263 (C), and Fc N459 (D). Determination of glycan composition was performed using Byonic software. The intensity of each ion peak was read from LC-MS and displayed in the graph, whose Byonic scores were more than 150 for N263-containing Fc peptides, 300 for N459-containing Fc peptides, and 250 for N49-containing J-chain peptides. For high intensity peaks, deduced structure(s) are shown on the top of each bar. The intensity was shown as the sum of the intensities from multiply charged peaks.

To examine the *N*-glycan composition of Fc and J-chain, IgA1-Fc and J-chain complexes (IgA1-Fc and J-chain, IgA-Fc and J-chain N49Q) were treated with trypsin and subjected to reverse-phase HPLC analysis (Fig. 12A). Several fractions were applied to LC-MS and LC-MS/MS analysis and the RP-HPLC fraction eluted at 18-19 min was shown to contain the J-chain glycopeptide [E48-R58] containing N49. The glycopeptides derived from the Fc portion were also analyzed by LC-MS and LC-MS/MS analyses. The results are summarized in Fig. 12B-D. The *N*-glycan at N49 of the J-chain is relatively short and mostly of the biantennary complex-type without galactose. Pauchmannose and oligomannose structures ($Man_1GlcNAc_2$, $Man_3GlcNAc_2$, and $Man_5GlcNAc_2$) were identified. It should be noted that unglycosylated J-chain peptide [E48-7R58] was also detected with high intensity (6.7×10^8). This observation suggests that J-chain *N*-glycosylation at N49 is not essential for the assembly with IgA1-Fc. The *N*-glycan pattern at N459(Fc) in Fc-J-chain complex is similar to the *N*-glycan pattern in Fc, however pauch/oligomannnose structures ($Man_{3-7}GlcNAc_2$) were significant in the Fc-J-chain complex. The *N*-glycan pattern at N263(Fc) in the Fc-J-chain complex is also similar to the *N*-glycan pattern in Fc, but as observed in N263 glycosylation, the $Man_5GlcNAc_2$ structure is most prevalent in the Fc-J-chain complex. Therefore, oligo/high mannose glycans are more frequently found in the Fc-J-chain complex than in Fc alone. Furthermore, there is less galactosylation in the Fc-J-chain

complex than in Fc alone. Then, overall, the Fc-J-chain complex bears fewer processed *N*-glycans, while Fc without J-chain possesses more processed *N*-glycans. A logical conclusion is that processing glycosidase enzymes have limited access to the Fc-J-chain complex, whereas Fc without J-chain is monomeric and access is without steric hindrance.

3.7 Effect of Fc *N*-glycans on the formation of Fc/J-chain complex

A thermofluor assay was performed to examine the thermal stability of Fc-J-chain complexes using *N*-glycosylation mutants. As shown in Fig. 13A, a higher melting

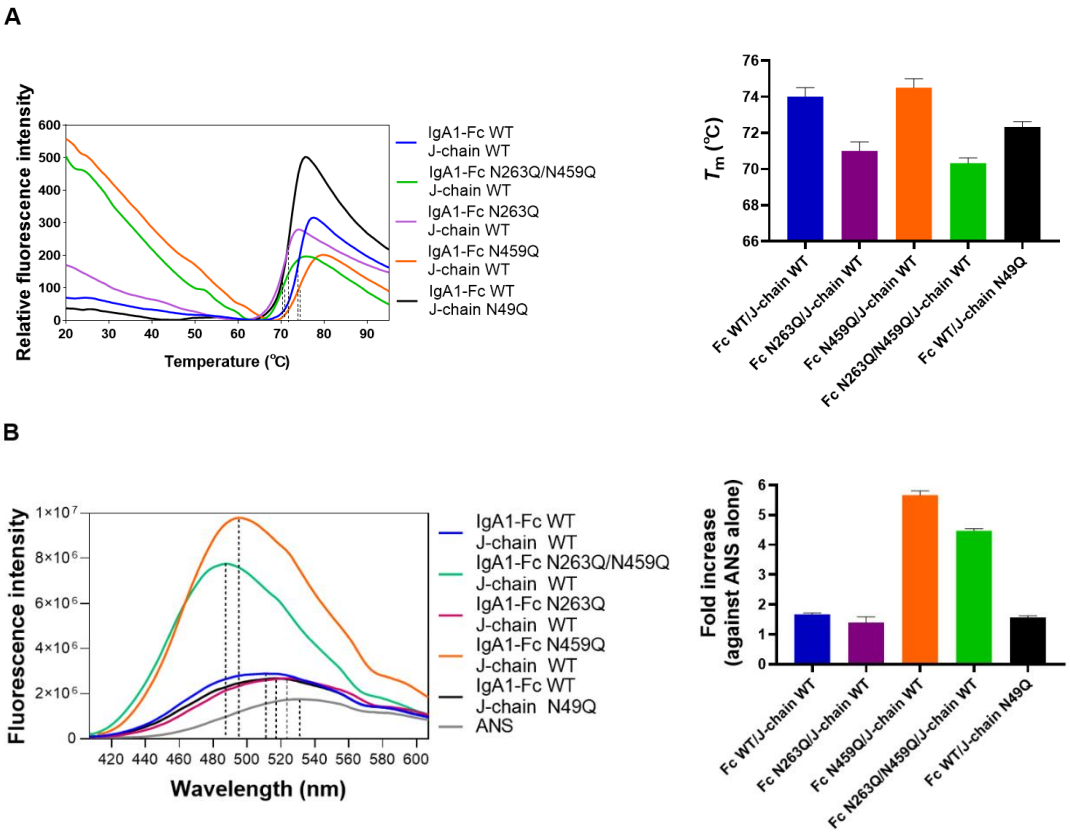

Figure 13. Analysis of thermal stability and surface hydrophobicity of IgA1-Fc-J-chain complexes using fluorescent probes.

(A) T_m measurement of IgA1-Fc-J-chain complexes by thermofluor assay using SYPRO Orange. Bar graph on the right shows T_m of each sample. The average T_m values are indicated with standard deviation from three independent experiments (n = 3). (B) Analysis of surface hydrophobicity using a fluorescent probe ANS. ANS fluorescence spectra were recorded in the presence or absence of IgA1-Fc-J-chain complex. Bar graph on the right shows the fold increase

of the maximum ANS fluorescence intensity in the presence of each mutant compared with that of ANS without protein with standard deviation from three independent experiments (n = 3).

temperature was observed for the wild-type complexes compared with that of IgA1-Fc alone. This indicates that the Fc part is stabilized when complexed with the J-chain. Melting temperatures of N263Q and N263Q/N459Q are significantly lower than that of wild-type, suggesting that N263-glycan contributes to the stability of the Fc-J-chain complex as well as of Fc alone. The T_m of the complex with J-chain N49Q (72.3 ℃) is lower than that of the complex with J-chain WT (74.0 ℃), suggesting that the J-chain *N*-glycan also contributes to the stabilization of the IgA1-Fc-J-chain complex. It is of note that both N459Q and N262Q/N459Q have relatively higher fluorescence intensity at 20°C. Based on this observation, we then performed ANS fluorescence assays of these complexes (Fig. 13B). We found that fluorescence of ANS is greatly enhanced in the presence of N459Q or the N262Q/N459Q complex and the wavelength giving maximum fluorescence intensity was blue-shifted. These data suggest the existence of a hydrophobic surface(s) around N459 at the tailpiece, which the *N*-glycans would cover, possibly preventing non-specific binding with another Fc molecule.

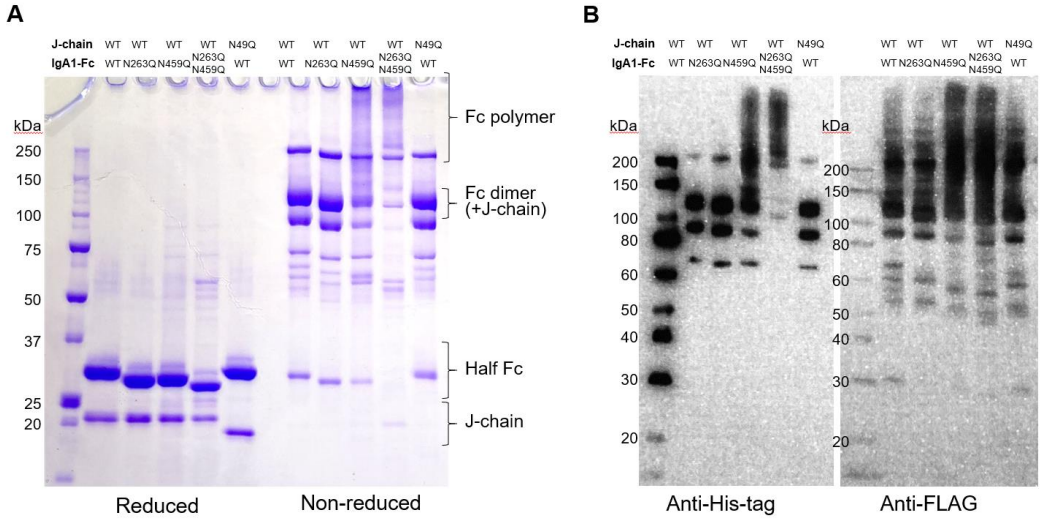

Figure 14. Effect of glycan composition on Fc/J-chain complex formation.

(A) SDS-PAGE of Fc/J-chain complex purified from the culture supernatant of Expi293F GnT-I(-) cells under reducing and non-reducing conditions. (B) Western blotting of the Fc/J-chain complexes performed under non-denaturing condition. The bands were detected with anti-

FLAG (detecting IgA1-Fc) or anti-His-tag (J-chain) antibodies.

Finally, to examine the effect of *N*-glycan composition on IgA1-Fc/J-chain assembly, stability and hydrophobicity, we produced IgA1-Fc and J-chain complexes with $Man_5GlcNAc_2$ glycan using an Expi293F GnT-I(-) cell line. The recombinant IgA1-Fc complexes (Fc WT/J-chain WT, Fc N263Q/J-chain WT, Fc N459Q/J-chain WT, Fc N263Q/N459Q/J-chain WT and Fc WT/J-chain N49Q) were first analyzed by SDS-PAGE under reducing and non-reducing conditions (Fig. 14A, 14B). Compared with Expi293F cells, IgA1-Fcs and J-chain from Expi293F GnT-I(-) cells showed sharper bands with slightly larger migrations under the reducing condition. Under the non-reducing condition, dimeric Fc with J-chain was observed at about ~130 kDa. Also, in this condition, some extra bands were detected with a molecular size less than 130 kDa.

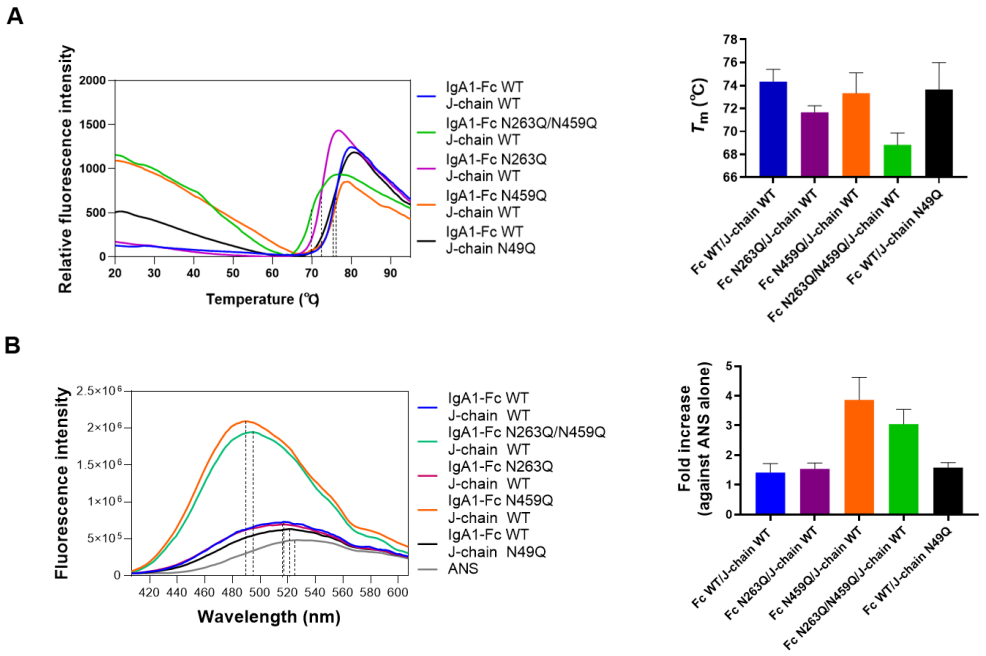

Figure 15. Thermal stability and surface hydrophobicity using Expi293F GnT-I(-) cells.
(A) The melting temperature (Tm) of Fc/J-chain complex from Expi293F GnT-I(-) cells. (B) Surface hydrophobicity of Fc/J-chain complex from Expi293F GnT-I(-) cells assessed using ANS fluorescence.

The presence of these bands suggests that the efficiency of IgA1-Fc/J-chain formation is only slightly affected by the composition of the *N*-glycan. IgA1-Fc/J-chain

complexes bearing $Man_5GlcNAc_2$ glycans were then analyzed by the thermofluor assay, and T_ms similar to those using Expi293F cells were obtained (Fig. 15A). This suggests that the glycan composition does not significantly affect the T_m of the complexes. The ANS fluorescence assay also suggested the exposure of a hydrophobic surface in N459Q-Man5 (Fig. 15B).

3.8 3D structural model of glycosylated Fc-J-chain complex

In the IgA1-Fc dimer, two Fc structural domains are close to their C-terminal ends, and the J-chain is asymmetrically located on one side of the dimer [5, 49]. To gain insight into the structural role of each *N*-glycan, we built a 3D structural model of glycosylated Fc-J-chain complex using the CHARMM-GUI [36] (Fig. 16A). As found in the crystal structure of the Fc-FcαR complex [50], the electron density of the *N*-glycan at N263 is well observed and the *N*-glycan extensively covers the Fc surface,

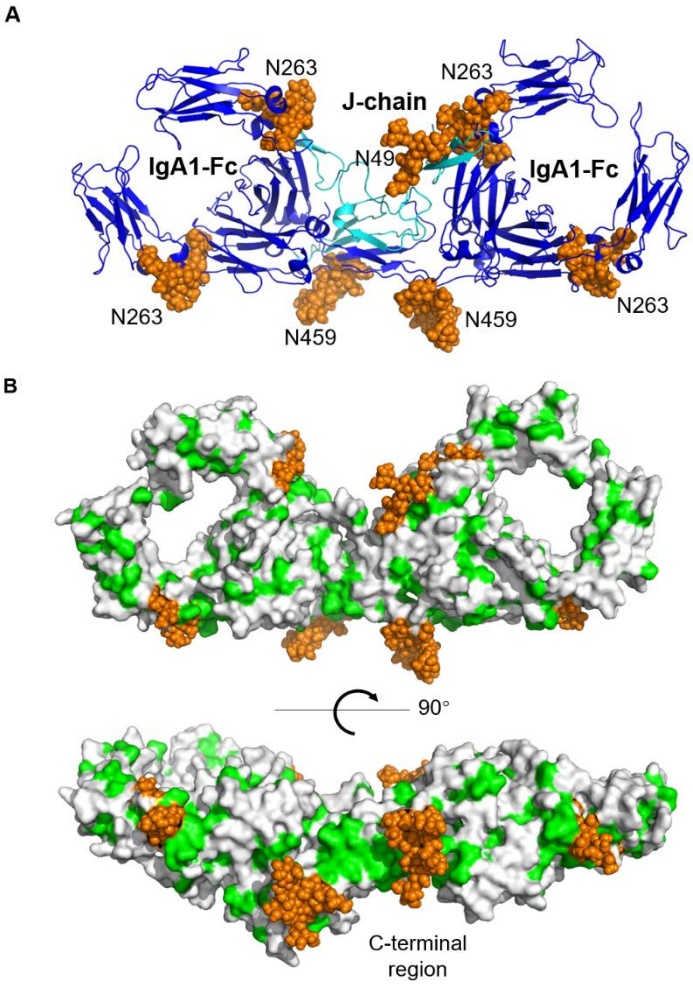

Figure 16. A 3D structural model of *N*-glycosylated IgA1-Fc-J-chain complex.

(A) 3D structural model of *N*-glycosylated Fc-J-chain complex built with Glycan Modeler tool in CHARMM-GUI [36] using the coordinates of dimeric sIgA complex (PDB ID: 6UE7). N263 and N49 of Fc and N49 of J-chain are artificially modeled with $Man_3GlcNAc_2$ structure. (B) Surface hydrophobicity of the model. Hydrophobic amino acid residues (F, A, V, L, I, P, W and M) are shown in green. Modeled *N*-glycans are shown in orange with sphere representation in (A) and (B). The figures were prepared using the PyMOL software.

thereby avoiding potential instability caused by the considerable surface exposure of the unpaired Cα2 domain [5, 10, 51]. N459 *N*-glycans are structurally clustered at the C-terminal tails of two Fc molecules and extend outside. This positioning likely prevents the formation of incorrect higher-order polymers, in accordance with a previous study [29]. It is of note that the C-terminal tails of the Fc molecules are highly hydrophobic, and it seems that clustered N459-glycans cover this surface (Fig. 16B). This is consistent with our ANS fluorescence results. It can also be speculated that the N459-glycans prevent another Fc molecule from approaching dimeric IgA. The *N*-glycans at N49 of the J-chain are located on the concave surface of the complex. It is possible that the *N*-glycan at N49 stabilizes the complex through intermolecular interaction with Fc. Further critical examination is needed for determination of the structural role of the *N*-glycan of the J-chain.

4. Conclusions

In conclusion, we successfully expressed and purified IgA1-Fc monomers and oligomers in the absence or presence of J-chain, verifying that J-chain is essential for the IgA1 multimerization. Our study shows more precisely the structure and function

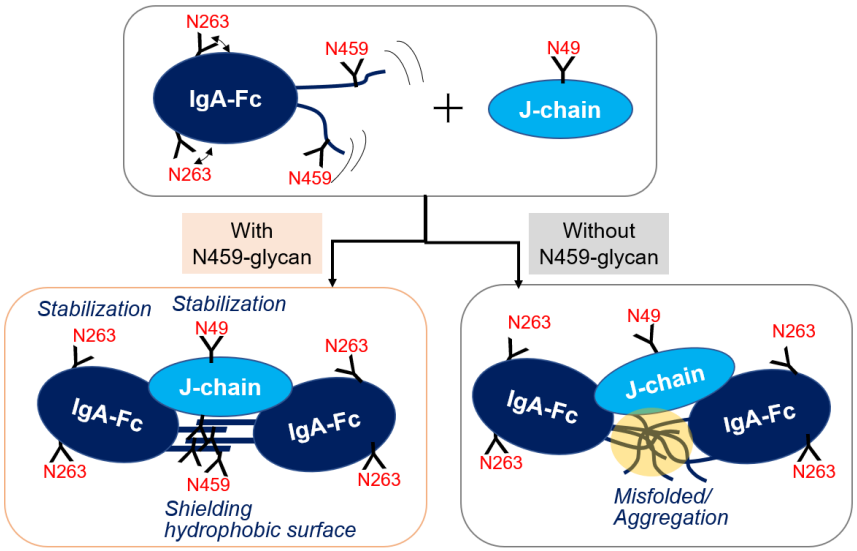

Figure 17. Proposed role of *N*-glycosylation on IgA and J-chain.

N459-glycan of IgA-Fc is not only required for its dimer assembly but also for inhibition of higher-order aggregates by covering the hydrophobic surface of the C-terminal tail. N263-glycan of IgA-Fc contributes to the stability of Fc through intramolecular glycan-polypeptide interaction. N49-glycan at J-chain also contributes to the stability of Fc-J-chain complex possibly by covering the negatively charged surface of the J-chain bound to Fc.

of the respective linked *N*-glycans at each glycosylation site. IgA1-Fc is site-specifically modified with *N*-glycans at different glycosylation sites, which play different roles in the formation of proper sIgA. N263-linked glycan affects the thermal stability of IgA1-Fc by interacting with the Fc and does not affect the production of monomeric or polymeric forms; however, N459-glycans promote the formation of proper IgA oligomers by covering hydrophobic surfaces at the tailpieces and inhibiting misfolding. Studies involving differential glycosylated species provide key insights for the design of medically important antibodies with optimal biological activity.

References

[1] P. de Sousa-Pereira, J.M. Woof, IgA: structure, function, and developability, Antibodies (Basel), 8 (2019) 57-86.

[2] J. Mestecky, M.W. Russell, S. Jackson, T.A. Brown, The human IgA system: a reassessment, Clin. Immunol. Immunopathol., 40 (1986) 105-114.

[3] P. Brandtzaeg, Role of J chain and secretory component in receptor-mediated glandular and hepatic transport of immunoglobulins in man, Scand. J. Immunol., 22 (1985) 111-146.

[4] T. Suzuki, A. Kawaguchi, A. Ainai, S. Tamura, R. Ito, P. Multihartina, V. Setiawaty, K.N. Pangesti, T. Odagiri, M. Tashiro, H. Hasegawa, Relationship of the quaternary structure of human secretory IgA to neutralization of influenza virus, Proc. Natl. Acad. Sc.i U. S. A., 112 (2015) 7809-7814.

[5] N. Kumar, C.P. Arthur, C. Ciferri, M.L. Matsumoto, Structure of the secretory immunoglobulin A core, Science, 367 (2020) 1008-1014.

[6] M.A. Otten, E. Rudolph, M. Dechant, C.W. Tuk, R.M. Reijmers, R.H. Beelen, J.G. van de Winkel, M. van Egmond, Immature neutrophils mediate tumor cell killing via IgA but not IgG Fc receptors, J. Immunol., 174 (2005) 5472-5280.

[7] Y. Guettinger, K. Barbin, M. Peipp, J. Bruenke, M. Dechant, H. Horner, D. Thierschmidt, T. Valerius, R. Repp, G.H. Fey, B. Stockmeyer, A recombinant bispecific single-chain fragment variable specific for HLA class II and FcαRI (CD89) recruits polymorphonuclear neutrophils for efficient lysis of malignant B lymphoid cells, J. Immunol., 184 (2010) 1210-1217.

[8] E.E. Olsan, T. Matsushita, M. Rezaei, T. Weimbs, Exploitation of the polymeric Immunoglobulin receptor for antibody targeting to renal cyst lumens in polycystic kidney disease, J. Biol. Chem., 290 (2015) 15679-15686.

[9] J.E. Bakema, M. van Egmond, Immunoglobulin A: A next generation of therapeutic antibodies?, MAbs, 3 (2011) 352-361.

[10] Y. Wang, G. Wang, Y. Li, Q. Zhu, H. Shen, N. Gao, J. Xiao, Structural insights into secretory immunoglobulin A and its interaction with a pneumococcal adhesin, Cell Res., 30 (2020) 602-609.

[11] S. Kumar Bharathkar, B.W. Parker, A.G. Malyutin, N. Haloi, K.E. Huey-Tubman, E. Tajkhorshid, B.M. Stadtmueller, The structures of secretory and dimeric immunoglobulin A, eLife, 9 (2020) e56098.

[12] M.J. Borrok, S.T. Jung, T.H. Kang, A.F. Monzingo, G. Georgiou, Revisiting the role of glycosylation in the structure of human IgG Fc, ACS Chem. Biol., 7 (2012) 1596-1602.

[13] R.L. Shields, J. Lai, R. Keck, L.Y. O'Connell, K. Hong, Y.G. Meng, S.H. Weikert, L.G. Presta, Lack of fucose on human IgG1 *N*-linked oligosaccharide improves binding to human FcγRIII and antibody-dependent cellular toxicity, J. Biol. Chem., 277 (2002) 26733-26740.

[14] L. Ding, X. Chen, H. Cheng, T. Zhang, Z. Li, Advances in IgA glycosylation and its correlation with diseases, Front Chem, 10 (2022) 974854.

[15] T.N. Lombana, S. Rajan, J.A. Zorn, D. Mandikian, E.C. Chen, A. Estevez, V. Yip, D.D. Bravo, W. Phung, F. Farahi, S. Viajar, S. Lee, A. Gill, W. Sandoval, J. Wang, C. Ciferri, C.A. Boswell, M.L. Matsumoto, C. Spiess, Production, characterization, and *in vivo* half-life extension of polymeric IgA molecules in mice, MAbs, 11 (2019) 1122-1138.

[16] S. Kawamura, N. Saitou, S. Ueda, Concerted evolution of the primate immunoglobulin α-gene through gene conversion, J. Biol. Chem., 267 (1992) 7359-7367.

[17] F.E. Johansen, R. Braathen, P. Brandtzaeg, Role of J chain in secretory immunoglobulin formation, Scand. J. Immunol., 52 (2000) 240-248.

[18] A. Mathias, B. Corthésy, Recognition of gram-positive intestinal bacteria by hybridoma- and colostrum-derived secretory immunoglobulin A is mediated by carbohydrates, J. Biol. Chem., 286 (2011) 17239-17247.

[19] A. Nakajima, A. Vogelzang, M. Maruya, M. Miyajima, M. Murata, A. Son, T. Kuwahara, T. Tsuruyama, S. Yamada, M. Matsuura, H. Nakase, D.A. Peterson, S. Fagarasan, K. Suzuki, IgA regulates the composition and metabolic function of gut microbiota by promoting symbiosis between bacteria, J. Exp. Med., 215 (2018) 2019-

2034.

[20] C. Perrier, N. Sprenger, B. Corthesy, Glycans on secretory component participate in innate protection against mucosal pathogens, J. Biol. Chem., 281 (2006) 14280-14287.

[21] L. Royle, A. Roos, D.J. Harvey, M.R. Wormald, D. van Gijlswijk-Janssen, R.M. Redwan el, I.A. Wilson, M.R. Daha, R.A. Dwek, P.M. Rudd, Secretory IgA *N*- and *O*-glycans provide a link between the innate and adaptive immune systems, J. Biol. Chem., 278 (2003) 20140-20153.

[22] A. Cravioto, A. Tello, H. Villafan, J. Ruiz, S. del Vedovo, J.R. Neeser, Inhibition of localized adhesion of enteropathogenic *Escherichia coli* to HEp-2 cells by immunoglobulin and oligosaccharide fractions of human colostrum and breast milk, J. Infect. Dis., 163 (1991) 1247-1255.

[23] H. Schroten, C. Stapper, R. Plogmann, H. Köhler, J. Hacker, F.G. Hanisch, Fab-independent antiadhesion effects of secretory immunoglobulin A on S-fimbriated *Escherichia coli* are mediated by sialyloligosaccharides, Infect. Immun., 66 (1998) 3971-3973.

[24] G.J. Rouwendal, M.M. van der Lee, S. Meyer, K.R. Reiding, J. Schouten, G. de Roo, D.F. Egging, J.H. Leusen, P. Boross, M. Wuhrer, G.F. Verheijden, W.H. Dokter, M. Timmers, R. Ubink, A comparison of anti-HER2 IgA and IgG1 in vivo efficacy is facilitated by high N-glycan sialylation of the IgA, MAbs, 8 (2016) 74-86.

[25] B.D. Oortwijn, A. Roos, P.J. van der Boog, N. Klar-Mohamad, A. van Remoortere, A.M. Deelder, M.R. Daha, C. van Kooten, Monomeric and polymeric IgA show a similar association with the myeloid FcαRI/CD89, Mol. Immunol., 44 (2007) 966-973.

[26] L. Carayannopoulos, E.E. Max, J.D. Capra, Recombinant human IgA expressed in insect cells, Proc Natl Acad Sci U S A, 91 (1994) 8348-8352.

[27] M.M. Gomes, S.B. Wall, K. Takahashi, J. Novak, M.B. Renfrow, A.B. Herr, Analysis of IgA1 *N*-glycosylation and its contribution to FcαRI binding, Biochemistry, 47 (2008) 11285-11299.

[28] M.A. Maurer, L. Meyer, M. Bianchi, H.L. Turner, N.P.L. Le, M. Steck, A.

Wyrzucki, V. Orlowski, A.B. Ward, M. Crispin, L. Hangartner, Glycosylation of human IgA directly inhibits influenza a and other sialic-acid-binding viruses, Cell Rep, 23 (2018) 90-99.

[29] P.D. Chuang, S.L. Morrison, Elimination of *N*-linked glycosylation sites from the human IgA1 constant region: effects on structure and function, J. Immunol, 158 (1997) 724-732.

[30] S. Krugmann, R.J. Pleass, J.D. Atkin, J.M. Woof, Mutagenesis of J chain residues critical for IgA dimer assembly, Biochem. Soc. Trans., 25 (1997) 323S.

[31] S. Pan, N. Manabe, Y. Yamaguchi, 3D structures of IgA, IgM, and components, Int. J. Mol. Sci., 22 (2021) 12776.

[32] J.V. Olsen, B. Macek, O. Lange, A. Makarov, S. Horning, M. Mann, Higher-energy C-trap dissociation for peptide modification analysis, Nat. Methods, 4 (2007) 709-712.

[33] M. Bern, Y.J. Kil, C. Becker, Byonic: advanced peptide and protein identification software, Curr Protoc Bioinformatics, Chapter 13 (2012) 13 20 11-13 20 14.

[34] S. Neelamegham, K. Aoki-Kinoshita, E. Bolton, M. Frank, F. Lisacek, T. Lütteke, N. O'Boyle, N.H. Packer, P. Stanley, P. Toukach, A. Varki, R.J. Woods, T.S.D. Group, Updates to the Symbol Nomenclature for Glycans guidelines, Glycobiology, 29 (2019) 620-624.

[35] M. Nagae, A. Ikeda, M. Hane, S. Hanashima, K. Kitajima, C. Sato, Y. Yamaguchi, Crystal structure of anti-polysialic acid antibody single chain Fv fragment complexed with octasialic acid: insight into the binding preference for polysialic acid, J. Biol. Chem., 288 (2013) 33784-33796.

[36] S.-J. Park, J. Lee, Y. Qi, N.R. Kern, H.S. Lee, S. Jo, I. Joung, K. Joo, J. Lee, W. Im, CHARMM-GUI Glycan Modeler for modeling and simulation of carbohydrates and glycoconjugates, Glycobiology, 29 (2019) 320-331.

[37] S. Jo, W. Im, Glycan fragment database: a database of PDB-based glycan 3D structures, Nucleic Acids Res., 41 (2012) D470-D474.

[38] O. Guvench, E. Hatcher, R.M. Venable, R.W. Pastor, A.D. MacKerell, Jr., CHARMM Additive All-Atom Force Field for Glycosidic Linkages between

Hexopyranoses, Journal of Chemical Theory and Computation, 5 (2009) 2353-2370.
[39] M. Tomana, W. Niedermeier, J. Mestecky, F. Skvaril, The differences in carbohydrate composition between the subclasses of IgA immunoglobulins, Immunochemistry, 13 (1976) 325-328.
[40] C.Y. Liew, J.-L. Chen, C.-K. Ni, Electrospray ionization in-source decay of N-glycans and the effects on N-glycan structural identification, Rapid Communications in Mass Spectrometry, 36 (2022) e9352.
[41] C. Grünwald-Gruber, A. Thader, D. Maresch, T. Dalik, F. Altmann, Determination of true ratios of different N-glycan structures in electrospray ionization mass spectrometry, Anal. Bioanal. Chem., 409 (2017) 2519-2530.
[42] A. Tanaka, H. Iwase, Y. Hiki, T. Kokubo, I. Ishii-Karakasa, K. Toma, Y. Kobayashi, K. Hotta, Evidence for a site-specific fucosylation of N-linked oligosaccharide of immunoglobulin A1 from normal human serum, Glycoconj J, 15 (1998) 995-1000.
[43] T.S. Mattu, R.J. Pleass, A.C. Willis, M. Kilian, M.R. Wormald, A.C. Lellouch, P.M. Rudd, J.M. Woof, R.A. Dwek, The glycosylation and structure of human serum IgA1, Fab, and Fc regions and the role of N-glycosylation on Fcalpha receptor interactions, J Biol Chem, 273 (1998) 2260-2272.
[44] K. Göritzer, D. Maresch, F. Altmann, C. Obinger, R. Strasser, Exploring site-specific N-glycosylation of HEK293 and plant-produced human IgA isotypes, J. Proteome Res., 16 (2017) 2560-2570.
[45] A. Hawe, M. Sutter, W. Jiskoot, Extrinsic fluorescent dyes as tools for protein characterization, Pharm. Res., 25 (2008) 1487-1499.
[46] A.W. Barb, J.H. Prestegard, NMR analysis demonstrates immunoglobulin G N-glycans are accessible and dynamic, Nat. Chem. Biol., 7 (2011) 147-153.
[47] K. Kato, Y. Yamaguchi, Y. Arata, Stable-isotope-assisted NMR approaches to glycoproteins using immunoglobulin G as a model system, Progress in nuclear magnetic resonance spectroscopy, 56 (2010) 346-359.
[48] Y. Yamaguchi, K. Kato, M. Shindo, S. Aoki, K. Furusho, K. Koga, N. Takahashi, Y. Arata, I. Shimada, Dynamics of the carbohydrate chains attached to the Fc portion

of immunoglobulin G as studied by NMR spectroscopy assisted by selective 13C labeling of the glycans, J. Biomol. NMR, 12 (1998) 385-394.

[49] A. Feinstein, E.A. Munn, N.E. Richardson, The three-dimensional conformation of M and A globulin molecules, Ann. N. Y. Acad. Sci., 190 (1971) 104-121.

[50] A.B. Herr, E.R. Ballister, P.J. Bjorkman, Insights into IgA-mediated immune responses from the crystal structures of human FcαRI and its complex with IgA1-Fc, Nature, 423 (2003) 614-620.

[51] G.K. Hui, D.W. Wright, O.L. Vennard, L.E. Rayner, M. Pang, S.C. Yeo, J. Gor, K. Molyneux, J. Barratt, S.J. Perkins, The solution structures of native and patient monomeric human IgA1 reveal asymmetric extended structures: implications for function and IgAN disease, Biochem. J., 471 (2015) 167-185.

Abbreviations

IgA: Immunoglobulin A

J-chain: joining chain

SC: secretory component

pIgR: polymeric Ig receptor

sIgA: secretory IgA

BsAb: bispecific antibodies

EPEC: enteropathogenic *Escherichia coli*

PBS: phosphate-buffered saline

CBB: Coomassie Brilliant Blue

TFA: trifluoroacetic acid

HCD: Higher-energy C-trap dissociation

FDR: false-discovery rate

SNFG: Symbol Nomenclature for Glycans

T_m: melting temperature

ANS: 8-anilino-1-naphthalenesulfonic acid

PHA-L4: *Phaseolus vulgaris* leucoagglutinin

PHA-E4: *Phaseolus vulgaris* erythroagglutinin

MAM: *Maackia amurensis*

SSA: *Sambucus sieboldiana*

AAL: *Aleuria aurantia* lectin

SEC: size exclusion chromatography

Acknowledgments

First of all, I owe my sincerely gratitude to President Motoaki Takayanagi and Prof. Jianguo Gu to provide the opportunity of studying in Tohoku Medical and Pharmaceutical University. I am a recipient of a special scholarship from Tohoku Medical and Pharmaceutical University, a scholarship from the Tohoku Kaihatsu Memorial Foundation and a scholarship from JEES for coronavirus. I really appreciate that they provided me with these scholarships to ensure that I can focus on my studies in Japan without worrying about money.

My sincere and hearty thanks and appreciations go firstly to my supervisor, Prof. Yoshiki Yamaguchi, whose suggestions and encouragement have given me much insight into these glycoprotein studies. It has been a great privilege and joy to study under his guidance and supervision. Furthermore, it is my honor to benefit from his personality and diligence, which I will treasure my whole life. This thesis would not have been possible unless Prof. Yamaguchi designed the project, analyzed the data and revised the manuscript. My gratitude to him knows no bounds.

I would love to appreciate my tutor, Dr. Noriyoshi Manabe, who is a very learned and responsible teacher in our Lab of Structural Glycobiology in this university. After every day's tiring and busy work of his own, he still devoted his considerate care and immense vigor to the supervision of my experiment design and handling, including his suggestions on writing thesis, his help in forming the structure, and the efforts to the refinement of my ideas in my thesis.

I also want to thank my teammates, for their friendly assistance and punctual information that helped me through the whole process of the thesis writing. Many thanks for Shiho Sasaki to help me with my life when I first came to Japan and for her technical help with computers. Especially, I would like to thank Ms. Hsiaoho Chou and Ms. Xiao Xu for their language and life support during my illness. I am very grateful

to Ms. Kokubu, Ms. Okada, and Ms. Chiba in the lab, etc., for taking me to learn about Japanese culture and experience Japanese food, and making it possible for me to study here happily

Finally, I would like to give my heartfelt thanks to my parents, for their endless love and care for me. Whatever I need and wherever I go, they are always there supporting me without any requirement in return. I thank my loving family and family is where I can forever turn.